Vaccination and immigration rates influence raccoon rabies elimination and recolonization in simulated urban-suburban landscapes

Emily M. Beasley[1] and Timothée Poisot[1]

[1]Département de Sciences Biologiques, Université de Montréal, Montréal, Québec, Canada

Correspondence: Emily M. Beasley, beasley.em@gmail.com

Abstract

The raccoon variant of the rabies virus (RRV) is managed in the eastern United States and Canada via distribution of oral rabies vaccine (ORV) baits. The goal of ORV distribution is to reach seroprevalence rates (an index of population immunity) of at least 60%, the threshold thought to eliminate RRV. Seroprevalence rates in urban areas rarely reach target levels, predictably leading to rabies outbreaks. However, many urban areas have spent several years rabies-free, aligning with previous work suggesting RRV can be eliminated from urban areas at below-target seroprevalence rates. Using an agent-based model to simulate raccoon populations in urban landscapes, we examined 1) whether RRV can be eliminated at vaccination thresholds below 60% and 2) whether landscapes with below-target vaccination rates are vulnerable to RRV recolonization, and 3) whether the rate and timing of immigration influences elimination and recolonization. Vaccination and immigration rates influenced elimination probability: elimination was more likely and occurred more quickly in landscapes with higher vaccination rates and less likely in landscapes with higher immigration rates. All immigration variables (immigration rate, immigrant disease prevalence, and immigration timing) influenced the probability of recolonization after rabies was eliminated: recolonization was more likely in landscapes with high immigration rates and when immigrants had higher disease prevalence, but less likely when

immigration occurred seasonally rather than continuously. Vaccination did not have a clear effect on recolonization probability but reduced the number of rabies cases during a recolonization event. Although elimination was highly likely in our simulated landscapes due to their small spatial extent, our results suggest that vaccination rates of at least 50% result in timely rabies elimination (median 1.5 years). After elimination is achieved, strategies for preventing infected individuals from entering the rabies-free area are essential for preventing recolonization events, as vaccination rates had a much smaller effect on recolonization that immigration rates and timing. Understanding long-distance movements of host individuals is crucial for managing diseases such as rabies which likely persist at the regional scale.

Keywords: raccoon rabies, urban ecology, immigration, rabies management, agent-based models, landscape ecology

Introduction

Rabies lyssavirus remains a zoonosis of global concern for both wildlife and humans (Elmore et al., 2017; Rupprecht et al., 2002; Vercauteren et al., 2012). Transmitted primarily through direct contact with an infected individual, rabies is usually fatal once observable symptoms appear (Rupprecht et al., 2002). Because the primary mode of transmission is host-to-host contact, understanding of the movement ecology and social behavior of a given host species are essential for understanding rabies transmission. In the eastern United States and Canada, raccoons (*Procyon lotor*) are the primary reservoir of the raccoon variant of the rabies virus (RRV) and are the largest source of terrestrial wildlife cases (Elmore et al., 2017; Gilbert A, 2018). Due to their broad geographic range and high tolerance of human-altered habitats (Lotze

& Anderson, 1979; Randa & Yunger, 2006; Slate et al., 2020), along with wide variation in demography and behavior across habitats (Prange et al., 2004; Prange & Gehrt, 2004; Slate et al., 2020), understanding raccoon ecology as it relates to rabies dynamics is still an active area of management concern.

Raccoons are highly philopatric, and their within-year movement is often constrained to a home range that is typically 1–4 km^2 in rural areas (Rees et al., 2008; Rosatte et al., 2010). Interspecific contacts between raccoons with overlapping or neighboring home ranges are frequent, but short in duration (Hirsch et al., 2013). As a result, the majority of rabies cases in raccoon populations are transmitted locally, and transmission rates are thought to be relatively low (Smith et al., 2002). Empirical estimates of the effective transmission rate (R_e) of raccoon rabies are barely above the threshold required for disease persistence (~1–1.2, Biek et al., 2007; Fisher et al., 2018). Rabies persistence is therefore maintained at a regional scale (Mancy et al., 2022) through a combination of wave-front dynamics (Childs et al., 2000; Smith et al., 2002), infrequent long-distance movements by infected individuals (Mancy et al., 2022; Rees et al., 2013; Smith et al., 2002), and human-mediated translocation events (Hopken, Bjorklund, et al., 2025; Nadin-Davis et al., 2020; Trewby et al., 2017).

Since the 1990s, management of RRV has been largely successful in controlling the geographic spread of the virus due to a combination of enhanced surveillance and vaccination (Davis et al., 2021; Elmore et al., 2017; Kirby et al., 2017; Rosatte et al., 2009), especially distribution of oral rabies vaccines (ORV). In rural areas, ORV deployment appears to achieve target seroprevalence rates (60–80%, Gilbert et al., 2018; Johnson et al., 2021) thought to be needed for RRV elimination (McClure et al., 2020; Rees et al., 2013; Reynolds et al., 2015). Despite the success of ORV campaigns in rural areas, vaccination campaigns have proven

challenging in urban and suburban landscapes, with seroprevalence rates typically falling below 40% (Beasley et al., 2024; Bigler et al., 2021; Mainguy et al., 2012). Urban and suburban raccoon populations often have very different demographics than their rural counterparts, including higher population densities, smaller home ranges, and differences in social behavior (Prange et al., 2003, 2004; Rosatte et al., 2010; Slate et al., 2020). Furthermore, urban habitats are often highly fragmented and can contain higher densities of nontarget bait competitors (e.g. virginia opossums *Didelphis virginiana*, feral cats *Felis catus*), which may influence the rate at which raccoons encounter ORV baits (Beasley et al., 2024). These ecological characteristics likely influence disease dynamics in urban and suburban areas, such as by increasing the duration of epizootics (Recuenco et al., 2007). Compounding the ecological challenges are logistical difficulties in bait distribution, resulting in bait distribution that is often along roads rather than in preferred urban raccoon habitat (Beasley et al., 2024; Bigler et al., 2021).

As a result of these challenges, ORV is much less effective in urban and suburban habitats, leading to chronically suboptimal seroprevalence rates (Bastille-Rousseau et al., 2024). Managers have developed strategies to increase the effectiveness of ORV campaigns, such as targeting preferred raccoon habitat (McClure et al., 2022), the use of bait stations in addition to hand baiting, and supplementing ORV distribution with trap-vaccinate-release (TVR) campaigns (Bastille-Rousseau et al., 2024). The use of TVR has proven particularly effective in increasing seroprevalence rates in urban landscapes, and its use in addition to ORV has resulted in significant reductions in rabies cases in Hamilton, Ontario (Bastille-Rousseau et al., 2024).

Despite low seroprevalence rates in urban areas, some vaccination campaigns have been successful in reaching local elimination (e.g. Burlington, VT, USA 2017–2022, Beasley et al., 2024; Ontario, Canada 2024, Ontario Ministry of Natural Resources and Forestry, 2025). The

reasons for this success are unclear. It is possible that seroprevalence rates lower than the current target of 60% are sufficient for elimination; particularly given the estimated effective reproduction number R_e is close to 1. However, a recent raccoon rabies outbreak in Burlington, Vermont ongoing since 2023 (Vermont Department of Health, 2025) suggests that low vaccination rates may leave urban and suburban areas particularly vulnerable to recolonization of the virus even if elimination has been achieved.

Understanding the role of vaccination rates, immigration rates, and the interaction between them is therefore critical for assessing how vulnerable urban areas are to rabies recolonization after the virus has been successfully eliminated. However, the relative paucity of raccoon movement data across the urban-rural gradient makes empirical assessments impossible. Agent-based models are a powerful tool for evaluating the effects of various factors on disease dynamics, as one can readily modify model parameters to explore their effects across a broad range of possible ecological conditions. Using a spatially explicit agent-based model applied to simulated landscapes, we explored the effect of vaccination and immigration on rabies elimination and re-colonization under varying vaccination rates. More specifically, we examined how 1) vaccination rates, 2) immigration rates, 3) rabies prevalence of immigrants, and 4) frequency of immigration (continuous vs. seasonal) impacted the probability and timing of rabies elimination and subsequent re-colonization. Based on previous work, we predict that rabies can be eliminated from landscapes with vaccination rates less than 60% (Acheson et al., 2023; Beasley et al., 2024), but that immigration will 1) increase the time it takes to successfully reach elimination by augmenting the susceptible population of raccoons, and 2) affect the probability of rabies re-colonization by influencing invasion pressure.

Materials and Methods

Full modeling methodology following the Overview, Design Concepts, Details (ODD) protocol for describing individual-based models (Grimm et al., 2006, 2010) can be found in Appendix 1.

Landscape Creation

We modeled urban-suburban landscapes by constructing 60 x 60 rasters using the package NeutralLandscapes.jl, which is based on the Python package NLMPy, in Julia 1.9.2 (Bezanson et al., 2017; Etherington et al., 2015; Poisot et al., 2023). Each grid cell was 0.5 x 0.5 km for a total landscape size of 30 km^2. We created habitat clusters using the mid-point displacement algorithm (Fournier et al., 1982), which takes as input an autocorrelation parameter. We used the function `lsm_l_ai` in the R package landscapemetrics (Hesselbarth et al., 2019) to calculate autocorrelation from land cover data from the greater Burlington, Vermont area (Homer et al., 2015). We re-classified the resulting raster into discrete habitat types, the relative proportions of which were derived from the Burlington land cover data. To prevent boundary effects (Koen et al., 2010), we also constructed a 5-cell buffer on each edge of the raster, resulting in a 50 x 50 grid of urban-suburban habitat surrounded by a unique "buffer" habitat.

Raccoon movement and demographics

Raccoon movement in the simulated landscapes was governed using weighted probabilities. At each time step, a raccoon could move to any of its eight neighboring cells or stay in its current cell. The probability of selecting a given cell was weighted according to a

habitat selection function, in which some habitats were more likely to be selected than others (McClure et al., 2022), a home range attractor, in which cells further from a raccoon's home cell were less likely to be selected as the destination cell (McClure et al., 2022; Signer et al., 2017), and conspecific avoidance. The home range attractor was calculated as a weighted probability:

$$p(\boldsymbol{c}_{t+1}) \propto \exp(-\omega \boldsymbol{d}(\boldsymbol{c}_{t+1})) \quad \text{(Eq. 1)}$$

In which $p(\boldsymbol{c}_{t+1})$ the probability of a raccoon occupying cell c within the raccoon's Moore neighborhood at time $t+1$, ω the strength of attraction towards the location of the home range attractor, and $\boldsymbol{d}(\boldsymbol{c}_t)$ the squared distance between potential target cells and the home cell. The squared distance between cells was calculated by:

$$\boldsymbol{d}(\boldsymbol{c}_{t+1}) = \frac{r\{(x_t - x_h)^2 + (y_t - y_h)^2\}}{100} \quad \text{(Eq. 2)}$$

In which (x_t, y_t) are x and y coordinates of the potential target cell, (x_h, y_h) are the x and y coordinates for the raccoon's home cell, and r is the resolution of each grid cell. Raccoons which had not reached the age of independence (20 weeks) always moved to the same cell as their mother (Viard et al., 2022). Raccoons could not move outside of the landscape boundaries unless they were dispersing (see below).

Raccoon demographics followed the literature where data is available (Appendix 2, Table 1). Female raccoons at least 52 weeks of age were considered eligible to reproduce, and the probability of reproduction in a given year was equal for all eligible raccoons. Births occurred in week 18 of each year of the simulation, with the litter size drawn from a Poisson distribution with an expected value (λ) of four. All raccoons were subject to stochastic mortality, in which the probability of mortality in a given week was 0.1%; old age mortality triggered at 416 weeks (eight years) of age; and density-related mortality which was triggered in cells with more than 10 raccoons (equivalent to 40 raccoons/km^2) and varied depending on the age of the raccoon

(Appendix 2, Table 1). In addition, raccoons younger than the age of independence were killed and removed from the simulation if their mother was dead.

Raccoons less than 1 year of age dispersed every year at week 43 of the simulation. For each dispersing raccoon, the direction of movement was determined by randomly selecting one of eight directions of movement corresponding to the cells surrounding the current cell (Cullingham et al., 2008). The raccoon then moved continuously in that direction for a given distance which was drawn from a Poisson distribution with an expected value (λ) of 3 cells (1.5 km, Rees et al., 2008): thus, it was possible for an agent to have a dispersal distance of 0 and remain in place. Dispersal was repeated until the agent either moved to a cell below carrying capacity or moved 3 total times, whichever occurred first. Raccoons over 1 year of age could also disperse, but only dispersed if they occupied a cell above carrying capacity, and had a smaller expected dispersal distance (λ = 2 cells or 1 km, Rees et al., 2008). Raccoons that left the landscape were removed from the simulation.

We simulated two types of raccoon immigration: a "consistent" type in which the landscape received a steady stream of a few immigrants per week, and a "seasonal" type in which the landscape received a much larger number of weekly immigrants in a specific time frame. In landscapes with consistent immigration, the number of weekly immigrants was drawn from a Poisson distribution with an expected value (λ) taking variable integer values ranging from 1–5. Landscapes with seasonal immigration had a weekly immigration rate drawn from a Poisson distribution with an expected value of $\lambda*5$, but immigration only occurred in weeks 40–50 to coincide with the annual dispersal period. In both cases, landscapes received approximately equal numbers of immigrants over the course of the simulation period. When entering the landscape, immigrants were assigned a direction of movement and a movement distance, the

185 latter of which was drawn from a Poisson distribution with an expected movement value (λ) of
186 10 cells. All immigrants were assumed to be susceptible to the disease. Although it is likely that
187 some raccoons immigrate from an ORV management zone and would have vaccine-induced
188 rabies immunity, the proportion of total immigrants represented by these individuals is unknown,
189 and we assumed full susceptibility to model a worst-case scenario. Immigrants were randomly
190 assigned an infected state as the outcome of a Bernoulli trial with varying probabilities of
191 success, ranging from 0–0.06 at intervals of 0.015.
192
193 *Disease dynamics.*
194 We modeled the disease as a spatially explicit SEIR model with additional demographic
195 processes as described above (Fig. 1). The spatially explicit component of the model primarily
196 affects the force of infection parameter λ, or the probability with which an infectious raccoon
197 infects a susceptible raccoon, which varies based on the proximity of each raccoon in a given
198 week. Infectious raccoons were assumed to be more likely to infect raccoons that were located
199 within 500 m of the infectious raccoon's current position (core home range transmission, λ_1 =
200 0.035) due to a high degree of overlap in weekly home ranges, and therefore a higher probability
201 of contact (Habib et al., 2011; Vander Wal et al., 2014, but see Yang et al., 2023). Susceptible
202 raccoons within 2 grid cells (1 km) of the infected raccoon were less likely to be infected (λ_2 =
203 0.02) due to a lower degree of home range overlap. Values of λ were selected based on the results
204 of a parameter sensitivity analysis (Appendix 2).
205 After a susceptible raccoon entered the exposed state, it could potentially recover from
206 the disease and acquire permanent immunity with a weekly probability of 0.002, which
207 corresponded to an 8–12% probability of recovery over the duration of the disease (Slate et al.,

2014). Raccoons which did not recover in a given week could transition to the infectious state with a probability $\delta \sim Beta(t, 5)$, in which t is the number of weeks the raccoon has spent in the exposed state. This results in a transition probability that increases over time, resulting in a typical incubation period of 4–6 weeks (Tinline et al., 2002). Raccoons in the infectious state always died after being infectious for 1 week (Hanlon et al., 2007).

Most agents transitioned to the recovered state via vaccination. Vaccination occurred during week 35 of the simulation, and the probability of vaccination was based on the agent's age and location. Agents in the buffer which were at least 1 year old had a vaccination probability of 60% (Fehlner-Gardiner et al., 2012). Agents elsewhere in the landscape that were at least 1 year old were vaccinated with a user-defined probability that ranged from 0–80% at 10% intervals. Agents less than 1 year old had a vaccination probability that was half of the probability for agents older than 1 year (Beasley et al., 2024). Once a raccoon entered the recovered state, it remained in that state (i.e. immunity was considered permanent).

Model specifications.

Raccoon populations were initialized with a mean population density of 6/km^2. Initial ages of the raccoons were randomly assigned with a possible range of 52–416 weeks (1–8 years). Raccoons were randomly assigned an initial vaccination status as the outcome of a Bernoulli trial with a probability of success that varied based on the adult vaccination rate assigned at the start of the simulation. The buffer zone of the simulation area was then populated at a density of 4/km^2 with a vaccination rate of 60%, with ages of the raccoons assigned as described above.

Rabies was introduced at the beginning of year two of the simulation to allow the raccoon population dynamics to stabilize. In each simulation, 10 susceptible raccoons were randomly

selected from the population to enter the exposed state. Disease dynamics then proceeded as described above.

Simulation replicates varied in adult vaccination rate, immigration type, immigration rate, and the proportion of immigrants that were infected (Appendix 2, Table 1). We ran 50 replicates of each combination of the above parameter values; each simulation ran for 11 years (one year to stabilize population + 10 years after rabies introduction). Data visualization was completed in R version 4.1.2 (R Core Team, 2021); R_0 and R_e were calculated using the R package `R0` (Boelle & Obadia, 2023). We compared 1) the probability of rabies elimination, 2) length of the initial outbreak, 3) weekly probability of recolonization, and 4) duration of subsequent outbreaks across our four variables. We defined a recolonization event as a period in which, after rabies was completely eliminated from the landscape, infected individuals were present in the landscape for a duration of at least 10 consecutive weeks. We chose a 10-week duration because, based on the latent period of the disease (Appendix 2, Figure 3), we can assume with near certainty that the disease was transmitted to at least one other individual. We compared weekly probability of recolonization rather than total probability because simulations in which elimination was achieved more rapidly had a longer time period in which rabies could potentially recolonize.

Results

Rabies was eliminated at least once in 86.7% of simulated landscapes, with an estimated R_0 of 1.38. The estimated value of R_e varied based on vaccination rates (Appendix 3, Figure 1) and varied temporally within simulations, but was typically 1.14 in simulations where the adult vaccination rate was 0%. Rabies prevalence varied between simulations and fluctuated

253 seasonally within each simulation, but was typically very low, with a maximum prevalence near
254 1.25% (Appendix 3, Fig. 2).
255 Elimination probability was strongly influenced by vaccination rates and weekly
256 immigration rate: increasing vaccination rates increased the likelihood of elimination, whereas
257 increased immigration rates increased the likelihood of rabies persistence (Fig. 2). Populations
258 with higher vaccination rates were also more resistant to the effects of increased immigration
259 rates: decreases in elimination probability due to increases in immigration rates were much lower
260 for populations with higher vaccination rates. Immigration type slightly influenced elimination
261 probability: simulations with seasonal immigration were slightly more likely to achieve
262 elimination than simulations with continuous immigration under the same vaccination rate
263 (Appendix 3, Fig. 3). There was also an interaction between immigration rate and immigrant
264 prevalence: rabies elimination was least likely when immigration rate and prevalence were both
265 high (Appendix 3, Fig. 4).
266 For simulations in which elimination was reached, elimination was achieved more
267 quickly in simulations with higher adult vaccination rates (Fig. 3). None of the immigration
268 variables had a clear effect on time to elimination.
269 For simulations in which rabies recolonization was possible (i.e., immigrant prevalence
270 was greater than 0 and rabies was eliminated at least once), total recolonization probability
271 ranged from 26.7% to 97.9%. All immigration variables influenced weekly recolonization
272 probability. Increasing immigration rates and immigrant prevalence resulted in increased weekly
273 colonization probability, and weekly probabilities were slightly lower when immigration
274 occurred seasonally rather than continuously (Fig. 4; Appendix 3, Fig. 5). Vaccination rates did
275 not have a clear effect on recolonization probability (Fig. 4).

Recolonization events were generally short in duration, typically lasting less than one year. There were no clear effects of any variables on the duration of recolonization events. When immigration was continuous, the timing of the recolonization event did not have a clear effect on outbreak duration (Appendix 3, Fig. 6). The number of cases after a recolonization event generally increased with immigration rates and decreased with vaccination rates (Appendix 3, Fig. 7).

Discussion

In line with our predictions, rabies elimination was possible at vaccination rates less than the target rate of 60%: in fact, elimination was common, occurring in more than 80% of simulations. The probability and speed of rabies elimination increased with increasing vaccination rates; whereas increased immigration rates resulted in lower probabilities of rabies elimination. Rabies elimination was likely facilitated by the relatively small extent of the simulated landscape and small raccoon home range sizes, as disease mortality and (when applicable) vaccination sufficiently reduced localized densities of susceptible individuals to reduce R_e below 1. Additionally, all of our immigration variables influenced rabies recolonization in a manner consistent with our predictions: higher immigration rates and higher disease prevalence in immigrants increased the likelihood of recolonization. Seasonal immigration was slightly less likely to result in rabies recolonization, likely due to a smaller time period in which recolonization is possible and due to the immigration period coinciding with the vaccination period. Vaccination rates had a very small influence on recolonization rates, but reduced the number of cases associated with recolonization events.

Our model, like all agent-based models, represents a simplified version of reality, the assumptions of which may impact the results. Our definition of "recolonization" essentially corresponded to an event in which an infected immigrant transmitted the virus to at least one other individual, which likely results in a recolonization probability that is much higher than the probability of a recolonization event leading to long-term persistence. However, defining the length of time corresponding to an "established" rabies outbreak would be somewhat arbitrary, and we chose a definition of "recolonization" that is more reproducible. Other modeling decisions, such as the grain size of the simulated landscapes and the use of a step function to model disease transmission, could have influenced the results (see Appendices 1–2 for more details on modeling decisions and the rationale behind them). It is possible that these decisions resulted in simulated enzootic periods that are shorter than empirical county-level enzootic periods (Childs et al., 2000), but our short enzootic periods could also be an artifact of the relatively small landscape extent. Given that our estimated R_e at vaccination rates of 0% is consistent with previous estimates of raccoon rabies R_e (Biek et al., 2007) and our estimated R_0 is consistent with estimates of R_0 among other rabies reservoirs (Hampson et al., 2009; Townsend et al., 2013; but see Li et al., 2024), our simulations are a sufficiently reasonable approximation of reality to produce useful results.

Our results suggest that, while vaccination rates at or above target levels offer some protection against recolonization events, they might not be sufficient to prevent recolonization entirely. This may be due to high raccoon population densities in urban areas (Prange et al., 2003, 2004; Rosatte et al., 2010; Slate et al., 2020): although many of our simulations had intentionally high proportions of vaccinated individuals, in terms of raw numbers, many agents were still susceptible to the disease. Furthermore, our choice of vaccination strategy may not be

the most efficient for rabies prevention: we assigned an equal vaccination probability for all adult agents in the simulation, whereas previous work suggests that targeting preferred habitat (where raccoons tend to congregate) is a more efficient vaccination strategy (McClure et al., 2022). Future work could investigate the efficacy of alternate vaccination strategies on preventing recolonization. Regardless, from a management perspective, vaccination is still an effective strategy for rabies elimination, and reducing the number of cases associated with potential recolonization events reduces the likelihood of dispersal of infected individuals to uninfected areas.

Due to longer enzootic periods as a result of low vaccination rates and susceptibility to rabies re-establishment, urban areas located within ORV management zones may increase the risk of a barrier breach by acting as a "stepping stone" to regions in which raccoon rabies has been eliminated. The standard width of ORV zones in the United States is 40 km (McClure et al., 2020), which is larger than the vast majority of recorded raccoon dispersal distances (Rosatte et al., 2010). However, an ORV zone width of 40 km may be insufficient when infected individuals disperse from within the ORV zone itself, due to a decrease in the distance an infected individual must travel to breach the barrier (McClure et al., 2020; Rees et al., 2013). The width of ORV zones that intersect an urban region may need to be increased to account for the possibility of long-distance movements that originate within the zone, particularly when the urban region is located in a known risk corridor that facilitates long-distance raccoon movement (Davis et al., 2019). Additional work is needed to assess the viability of urban areas as stepping stones and evaluate the ability of increased ORV zone width to counteract potential stepping stone effects.

The dynamics of rabies re-emergence in regions where it has been previously eliminated are highly dependent on the timing and intensity of raccoon movement, as well as the origin of

displaced raccoons. Immigrants from rural areas inside the ORV zone are more likely to be vaccinated than those from urban areas (Beasley et al., 2024; Bigler et al., 2021; Gilbert et al., 2018; Johnson et al., 2021; Mainguy et al., 2012), and may represent a high enough proportion of immigrants to reduce recolonization risk. Furthermore, our results demonstrate that the seasonality and intensity of immigration influence rabies dynamics. Given that raccoons are highly philopatric, with relatively short dispersal distances (Rees et al., 2008; Rosatte et al., 2010), immigration rates in this study are likely artificially high. However, the paucity of movement data across the urban-rural interface make it difficult to accurately model immigration timing, intensity, and origin. Previous work using genetic methods successfully identified the origin of three raccoons which had undergone long-distance translocations (Hopken, Bjorklund, et al., 2025); but due the lack of clear population structure at finer geographic scales (Hopken et al., 2023; Root et al., 2009; but see Hopken, Mankowski, et al., 2025) it is unclear if these methods be useful for quantifying movement across highly localized urban/rural gradients. More data are needed to understand raccoon movements in the urban-rural transition zone and the effects of these movements on rabies transmission.

Our results demonstrate that, even in urban and suburban landscapes with high raccoon population density, rabies elimination and subsequent recolonization is highly probable at small spatial extents. This work aligns with previous findings suggesting that local rabies transmission is relatively low and that persistence is maintained on a regional scale (Biek et al., 2007; Fisher et al., 2018; Mancy et al., 2022; Smith et al., 2002). However, urban and suburban areas still represent localized points of management concern, as the low vaccination rates in these areas increases their potential as “stepping stones” that reduce the distance required to breach the

vaccination barrier. The potential for urban areas to concentrate or amplify outbreak risk suggests the need for flexible, targeted management for both rabies elimination and prevention.

Acknowledgements. We thank Amy Davis and Kim Pepin for their helpful advice on our methodology. This research was funded by award 223764/Z/21/Z from the Wellcome Trust and a National Science Foundation (NSF) Biology Integration Institute grant (DBI 2213854) to the Verena program (viralemergence.org).

References

Acheson, E. S., Viard, F., Buchanan, T., Nituch, L., & Leighton, P. A. (2023). Comparing Control Intervention Scenarios for Raccoon Rabies in Southern Ontario between 2015 and 2025. *Viruses*, *15*(2), Article 2. https://doi.org/10.3390/v15020528

Bastille-Rousseau, G., Gorman, N. T., McClure, K. M., Nituch, L., Buchanan, T., Chipman, R. B., Gilbert, A. T., & Pepin, K. M. (2024). Assessing the Efficiency of Local Rabies Vaccination Strategies for Raccoons (Procyon lotor) in an Urban Setting. *Journal of Wildlife Diseases*, *60*(1). https://doi.org/10.7589/JWD-D-23-00059

Beasley, E. M., Nelson, K. M., Slate, D., Gilbert, A. T., Pogmore, F. E., Chipman, R. B., & Davis, A. J. (2024). Oral Rabies Vaccination of Raccoons (Procyon lotor) across a Development Intensity Gradient in Burlington, Vermont, USA, 2015–2017. *Journal of Wildlife Diseases*, *60*(1), 1–13. https://doi.org/10.7589/JWD-D-22-00117

Bezanson, J., Edelman, A., Karpinski, S., & Shah, V. B. (2017). Julia: A fresh approach to numerical computing. *SIAM Review*, *59*(1), 65–98.

Biek, R., Henderson, J. C., Waller, L. A., Rupprecht, C. E., & Real, L. A. (2007). A high-resolution genetic signature of demographic and spatial expansion in epizootic rabies

virus. *Proceedings of the National Academy of Sciences*, *104*(19), 7993–7998. https://doi.org/10.1073/pnas.0700741104

Bigler, L. L., Ochwat, J. B., Scarpitta, S. C., Matthews, B. W., Rudd, R. J., & Lein, D. H. (2021). Virus neutralizing antibody following oral rabies vaccination of raccoons (Procyon lotor) on suburban Long Island, New York, USA. *The Journal of Wildlife Diseases*, *57*(1), 145–156.

Boelle, P.-Y., & Obadia, T. (2023). *R0: Estimation of R0 and Real-Time Reproduction Number from Epidemics* (Version 1.3-1) [R]. https://cran.r-project.org/web/packages/R0/index.html

Childs, J. E., Curns, A. T., Dey, M. E., Real, L. A., Feinstein, L., Bjørnstad, O. N., & Krebs, J. W. (2000). Predicting the local dynamics of epizootic rabies among raccoons in the United States. *Proceedings of the National Academy of Sciences*, *97*(25), 13666–13671. https://doi.org/10.1073/pnas.240326697

Cullingham, C. I., Pond, B. A., Kyle, C. J., Rees, E. E., Rosatte, R. C., & White, B. N. (2008). Combining direct and indirect genetic methods to estimate dispersal for informing wildlife disease management decisions. *Molecular Ecology*, *17*(22), 4874–4886. https://doi.org/10.1111/j.1365-294X.2008.03956.x

Davis, A. J., Kirby, J. D., Chipman, R. B., Nelson, K. M., & Gilbert, A. T. (2021). Data-Driven Management—A Dynamic Occupancy Approach to Enhanced Rabies Surveillance Prioritization. *Viruses*, *13*(9), Article 9. https://doi.org/10.3390/v13091795

Davis, A. J., Nelson, K. M., Kirby, J. D., Wallace, R., Ma, X., Pepin, K. M., Chipman, R. B., & Gilbert, A. T. (2019). Rabies Surveillance Identifies Potential Risk Corridors and Enables Management Evaluation. *Viruses*, *11*(11), Article 11. https://doi.org/10.3390/v11111006

Elmore, S. A., Chipman, R. B., Slate, D., Huyvaert, K. P., VerCauteren, K. C., & Gilbert, A. T. (2017). Management and modeling approaches for controlling raccoon rabies: The road to elimination. *PLOS Neglected Tropical Diseases*, *11*(3), e0005249. https://doi.org/10.1371/journal.pntd.0005249

Etherington, T. R., Holland, E. P., & O'Sullivan, D. (2015). NLMpy: A python software package for the creation of neutral landscape models within a general numerical framework. *Methods in Ecology and Evolution*, *6*(2), 164–168. https://doi.org/10.1111/2041-210X.12308

Fehlner-Gardiner, C., Rudd, R., Donovan, D., Slate, D., Kempf, L., & Badcock, J. (2012). Comparing ONRAB And RABORAL V-RG oral rabies vaccine field performance in raccoons and striped skunks, New Brunswick, Canada, and Maine, USA. *Journal of Wildlife Diseases*, *48*(1), 157–167.

Fisher, C. R., Streicker, D. G., & Schnell, M. J. (2018). The spread and evolution of rabies virus: Conquering new frontiers. *Nature Reviews Microbiology*, *16*(4), 241–255. https://doi.org/10.1038/nrmicro.2018.11

Fournier, A., Fussell, D., & Carpenter, L. (1982). Computer rendering of stochastic models. *Communications of the ACM*, *25*(6), 371–384. https://doi.org/10.1145/358523.358553

Gilbert A, T. (2018). Rabies virus vectors and reservoir species. *Revue Scientifique et Technique (International Office of Epizootics)*, *37*(2), 371–384. https://doi.org/10.20506/rst.37.2.2808

Gilbert, A. T., Johnson, S. R., Nelson, K. M., Chipman, R. B., Algeo, T. P., Rupprecht, C. E., & Slate, D. (2018). Field trials of Ontario Rabies Vaccine bait in the northeastern USA, 2012–14. *Journal of Wildlife Diseases*, *54*(4), 790–801.

Grimm, V., Berger, U., Bastiansen, F., Eliassen, S., Ginot, V., Giske, J., Goss-Custard, J., Grand, T., Heinz, S. K., Huse, G., Huth, A., Jepsen, J. U., Jørgensen, C., Mooij, W. M., Müller, B., Pe'er, G., Piou, C., Railsback, S. F., Robbins, A. M., … DeAngelis, D. L. (2006). A standard protocol for describing individual-based and agent-based models. *Ecological Modelling*, *198*(1), 115–126. https://doi.org/10.1016/j.ecolmodel.2006.04.023

Grimm, V., Berger, U., DeAngelis, D. L., Polhill, J. G., Giske, J., & Railsback, S. F. (2010). The ODD protocol: A review and first update. *Ecological Modelling*, *221*(23), 2760–2768. https://doi.org/10.1016/j.ecolmodel.2010.08.019

Habib, T. J., Merrill, E. H., Pybus, M. J., & Coltman, D. W. (2011). Modelling landscape effects on density–contact rate relationships of deer in eastern Alberta: Implications for chronic wasting disease. *Ecological Modelling*, *222*(15), 2722–2732. https://doi.org/10.1016/j.ecolmodel.2011.05.007

Hampson, K., Dushoff, J., Cleaveland, S., Haydon, D. T., Kaare, M., Packer, C., & Dobson, A. (2009). Transmission Dynamics and Prospects for the Elimination of Canine Rabies. *PLoS Biology*, *7*(3), e1000053. https://doi.org/10.1371/journal.pbio.1000053

Hanlon, C. A., Niezgoda, M., & Rupprecht, C. E. (2007). 5—Rabies in Terrestrial Animals. In A. C. Jackson & W. H. Wunner (Eds.), *Rabies (Second Edition)* (pp. 201–258). Academic Press. https://doi.org/10.1016/B978-012369366-2/50007-5

Hesselbarth, M. H. K., Sciaini, M., With, K. A., Wiegand, K., & Nowosad, J. (2019). landscapemetrics: An open-source R tool to calculate landscape metrics. *Ecography*, *42*(10), 1648–1657. https://doi.org/10.1111/ecog.04617

Hirsch, B. T., Prange, S., Hauver, S. A., & Gehrt, S. D. (2013). Raccoon Social Networks and the Potential for Disease Transmission. *PLOS ONE*, *8*(10), e75830. https://doi.org/10.1371/journal.pone.0075830

Homer, C., Dewitz, J., Yang, L., Jin, S., Danielson, P., Xian, G., Coulston, J., Herold, N., Wickham, J., & Megown, K. (2015). Completion of the 2011 National Land Cover Database for the Conterminous United States – Representing a Decade of Land Cover Change Information. *Photogrammetric Engineering & Remote Sensing*, *81*(5), 345–354. https://doi.org/10.1016/S0099-1112(15)30100-2

Hopken, M. W., Bjorklund, B., Mankowski, C. C. P., Kirby, J., Chipman, R. B., Buchanan, T., Nituch, L., Gagnier, M., Massé, A., & Gilbert, A. T. (2025). Tracking the Origin of Raccoon (Procyon lotor) Translocations in Northeastern North America Using Population Genetics. *Northeastern Naturalist*, *31*(4), 539–554. https://doi.org/10.1656/045.031.0412

Hopken, M. W., Mankowski, C. P., Thurber, C., Piaggio, A. J., Nelson, K. M., Chipman, R. B., Abdo, Z., Buchanan, T., Massé, A., & Gilbert, A. T. (2025). Contrasting Patterns of

Raccoon (Procyon lotor) Spatial Population Genomics Throughout a Rabies Management Area in Eastern North America. *Evolutionary Applications*, *18*(5), e70105. https://doi.org/10.1111/eva.70105

Hopken, M. W., Piaggio, A. J., Abdo, Z., Chipman, R. B., Mankowski, C. P., Nelson, K. M., Hilton, M. S., Thurber, C., Tsuchiya, M. T. N., Maldonado, J. E., & Gilbert, A. T. (2023). Are rabid raccoons (Procyon lotor) ready for the rapture? Determining the geographic origin of rabies virus-infected raccoons using RADcapture and microhaplotypes. *Evolutionary Applications*, *16*(12), 1937–1955. https://doi.org/10.1111/eva.13613

Johnson, S. R., Slate, D., Nelson, K. M., Davis, A. J., Mills, S. A., Forbes, J. T., VerCauteren, K. C., Gilbert, A. T., & Chipman, R. B. (2021). Serological responses of raccoons and striped skunks to Ontario rabies vaccine bait in West Virginia during 2012–2016. *Viruses*, *13*(2), 157.

Kirby, J. D., Chipman, R. B., Nelson, K. M., Rupprecht, C. E., Blanton, J. D., Algeo, T. P., & Slate, D. (2017). Enhanced rabies surveillance to support effective oral rabies vaccination of raccoons in the eastern United States. *Tropical Medicine and Infectious Disease*, *2*(3), 34.

Li, M., Roswell, M., Hampson, K., Bolker, B. M., & Dushoff, J. (2024). *Reassessing global historical $\mathscr{R}_0$ estimates of canine rabies*. https://doi.org/10.1101/2024.04.11.589097

Lotze, J.-H., & Anderson, S. (1979). Procyon lotor. *Mammalian Species*, *119*, 1–8.

Mainguy, J., Rees, E. E., Canac-Marquis, P., Bélanger, D., Fehlner-Gardiner, C., Séguin, G., Larrat, S., Lair, S., Landry, F., & Côté, N. (2012). Oral rabies vaccination of raccoons and striped skunks with ONRAB® baits: Multiple factors influence field immunogenicity. *Journal of Wildlife Diseases*, *48*(4), 979–990.

Mancy, R., Rajeev, M., Lugelo, A., Brunker, K., Cleaveland, S., Ferguson, E. A., Hotopp, K., Kazwala, R., Magoto, M., Rysava, K., Haydon, D. T., & Hampson, K. (2022). Rabies shows how scale of transmission can enable acute infections to persist at low prevalence. *Science*, *376*(6592), 512–516. https://doi.org/10.1126/science.abn0713

McClure, K. M., Bastille-Rousseau, G., Davis, A. J., Stengel, C. A., Nelson, K. M., Chipman, R. B., Wittemyer, G., Abdo, Z., Gilbert, A. T., & Pepin, K. M. (2022). Accounting for animal movement improves vaccination strategies against wildlife disease in heterogeneous landscapes. *Ecological Applications*, *32*(4), e2568.

McClure, K. M., Gilbert, A. T., Chipman, R. B., Rees, E. E., & Pepin, K. M. (2020). Variation in host home range size decreases rabies vaccination effectiveness by increasing the spatial spread of rabies virus. *Journal of Animal Ecology*, *89*(6), 1375–1386. https://doi.org/10.1111/1365-2656.13176

Nadin-Davis, S., Buchanan, T., Nituch, L., & Fehlner-Gardiner, C. (2020). A long-distance translocation initiated an outbreak of raccoon rabies in Hamilton, Ontario, Canada. *PLOS Neglected Tropical Diseases*, *14*(3), e0008113. https://doi.org/10.1371/journal.pntd.0008113

Ontario Ministry of Natural Resources and Forestry. (2025, April 14). *Wildlife rabies outbreaks and control operations*. http://www.ontario.ca/page/wildlife-rabies-outbreaks-and-control-operations

Poisot, T., Borregaard, M. K., Catchen, M. D., Schouten, R., & Baudrot, V. (2023). *NeutralLandscapes* (Version 0.1.3) [Julia]. https://docs.ecojulia.org/NeutralLandscapes.jl/dev/

Prange, S., & Gehrt, S. D. (2004). Changes in mesopredator-community structure in response to urbanization. *Canadian Journal of Zoology*, *82*(11), 1804–1817. https://doi.org/10.1139/z04-179

Prange, S., Gehrt, S. D., & Wiggers, E. P. (2003). Demographic factors contributing to high raccoon densities in urban landscapes. *The Journal of Wildlife Management*, 324–333.

Prange, S., Gehrt, S. D., & Wiggers, E. P. (2004). Influences of anthropogenic resources on raccoon (Procyon lotor) movements and spatial distribution. *Journal of Mammalogy*, *85*(3), 483–490.

Randa, L. A., & Yunger, J. A. (2006). Carnivore occurrence along an urban-rural gradient: A landscape-level analysis. *Journal of Mammalogy*, *87*(6).

Recuenco, S., Eidson, M., Kulldorff, M., Johnson, G., & Cherry, B. (2007). Spatial and temporal patterns of enzootic raccoon rabies adjusted for multiple covariates. *International Journal of Health Geographics*, *6*(1), 14. https://doi.org/10.1186/1476-072X-6-14

Rees, E. E., Pond, B. A., Phillips, J. R., & Murray, D. (2008). Raccoon ecology database: A resource for population dynamics modelling and meta-analysis. *Ecological Informatics*, *3*(1), 87–96. https://doi.org/10.1016/j.ecoinf.2008.01.002

Rees, E. E., Pond, B. A., Tinline, R. R., & Bélanger, D. (2013). Modelling the effect of landscape heterogeneity on the efficacy of vaccination for wildlife infectious disease control. *Journal of Applied Ecology*, *50*(4), 881–891. https://doi.org/10.1111/1365-2664.12101

Reynolds, J. J. H., Hirsch, B. T., Gehrt, S. D., & Craft, M. E. (2015). Raccoon contact networks predict seasonal susceptibility to rabies outbreaks and limitations of vaccination. *Journal of Animal Ecology*, *84*(6), 1720–1731. https://doi.org/10.1111/1365-2656.12422

Root, J. J., Puskas, R. B., Fischer, J. W., Swope, C. B., Neubaum, M. A., Reeder, S. A., & Piaggio, A. J. (2009). Landscape Genetics of Raccoons (Procyon lotor) Associated with Ridges and Valleys of Pennsylvania: Implications for Oral Rabies Vaccination Programs. *Vector-Borne and Zoonotic Diseases*, *9*(6), 583–588. https://doi.org/10.1089/vbz.2008.0110

Rosatte, R., Donovan, D., Allan, M., Bruce, L., Buchanan, T., Sobey, K., Stevenson, B., Gibson, M., MacDonald, T., Whalen, M., Davies, J. C., Muldoon, F., & Wandeler, A. (2009). The control of raccoon rabies in Ontario, Canada: Proactive and reactive tactics, 1994–2007. *Journal of Wildlife Diseases*, *45*, 772–784.

Rosatte, R., Ryckman, M., Ing, K., Proceviat, S., Allan, M., Bruce, L., Donovan, D., & Davies, J. C. (2010). Density, movements, and survival of raccoons in Ontario, Canada: Implications for disease spread and management. *Journal of Mammalogy*, *91*(1), 122–135. https://doi.org/10.1644/08-MAMM-A-201R2.1

Rupprecht, C. E., Hanlon, C. A., & Hemachudha, T. (2002). Rabies re-examined. *The Lancet Infectious Diseases*, *2*(6), 327–343. https://doi.org/10.1016/S1473-3099(02)00287-6

Signer, J., Fieberg, J., & Avgar, T. (2017). Estimating utilization distributions from fitted step-selection functions. *Ecosphere*, *8*(4), e01771. https://doi.org/10.1002/ecs2.1771

Slate, D., Chipman, R. B., Algeo, T. P., Mills, S. A., Nelson, K. M., Croson, C. K., Dubovi, E. J., Vercauteren, K., Renshaw, R. W., Atwood, T., Johnson, S., & Rupprecht, C. E. (2014). Safety and immunogenicity of Ontario Rabies Vaccine Bait (ONRAB) in the first US field trial in raccoons (Procyon lotor). *Journal of Wildlife Diseases*, *50*(3), 582–595. https://doi.org/10.7589/2013-08-207

Slate, D., Saidy, B. D., Simmons, A., Nelson, K. M., Davis, A., Algeo, T. P., Elmore, S. A., & Chipman, R. B. (2020). Rabies Management Implications Based on Raccoon Population Density Indexes. *The Journal of Wildlife Management*, *84*(5), 877–890. https://doi.org/10.1002/jwmg.21869

Smith, D. L., Lucey, B., Waller, L. A., Childs, J. E., & Real, L. A. (2002). Predicting the spatial dynamics of rabies epidemics on heterogeneous landscapes. *Proceedings of the National Academy of Sciences*, *99*(6), 3668–3672. https://doi.org/10.1073/pnas.042400799

Tinline, R., Rosatte, R., & MacInnes, C. (2002). Estimating the incubation period of raccoon rabies: A time–space clustering approach. *Preventive Veterinary Medicine*, *56*(1), 89–103. https://doi.org/10.1016/S0167-5877(02)00126-5

Townsend, S. E., Sumantra, I. P., Pudjiatmoko, Bagus, G. N., Brum, E., Cleaveland, S., Crafter, S., Dewi, A. P. M., Dharma, D. M. N., Dushoff, J., Girardi, J., Gunata, I. K., Hiby, E. F., Kalalo, C., Knobel, D. L., Mardiana, I. W., Putra, A. A. G., Schoonman, L., Scott–Orr, H., … Hampson, K. (2013). Designing Programs for Eliminating Canine Rabies from Islands: Bali, Indonesia as a Case Study. *PLOS Neglected Tropical Diseases*, *7*(8), e2372. https://doi.org/10.1371/journal.pntd.0002372

Trewby, H., Nadin-Davis, S. A., Real, L. A., & Biek, R. (2017). Processes Underlying Rabies Virus Incursions across US–Canada Border as Revealed by Whole-Genome

Phylogeography. *Emerging Infectious Diseases*, *23*, 1454–1461. https://doi.org/10.3201/eid2309.170325

Vander Wal, E., Laforge, M. P., & McLoughlin, P. D. (2014). Density dependence in social behaviour: Home range overlap and density interacts to affect conspecific encounter rates in a gregarious ungulate. *Behavioral Ecology and Sociobiology*, *68*(3), 383–390. https://doi.org/10.1007/s00265-013-1652-0

Vercauteren, K. C., Ellis, C., Chipman, R., DeLiberto, T. J., Shwiff, S. A., & Slate, D. (2012). Rabies in North America: A Model of the One Health Approach. *Wildlife Diseases*.

Vermont Department of Health. (2025, March). *2024 Rabies Surveillance Report*. https://www.healthvermont.gov/sites/default/files/document/lsid-2024-rabies-surveillance-report.pdf

Viard, F., Acheson, E., Allibert, A., Sauve, C., & Leighton, P. (2022). *SamPy: A New Python Library for Stochastic Spatial Agent-Based Modeling in Epidemiology of Infectious Diseases* (2022110556). Preprints. https://doi.org/10.20944/preprints202211.0556.v2

Yang, A., Boughton, R., Miller, R. S., Snow, N. P., Vercauteren, K. C., Pepin, K. M., & Wittemyer, G. (2023). Individual-level patterns of resource selection do not predict hotspots of contact. *Movement Ecology*, *11*(1), 74. https://doi.org/10.1186/s40462-023-00435-9

Figures and Tables

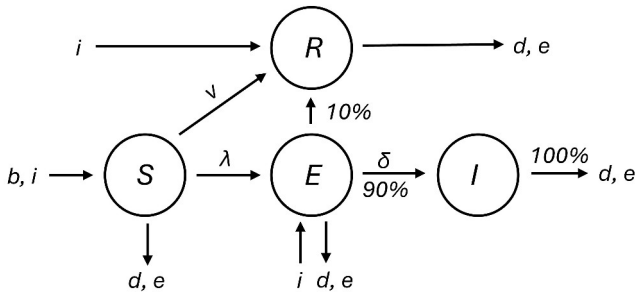

379 **Figure 1.** Transitions between susceptible (S), exposed (E), infected (I), and recovered (R)
380 disease states of the model. Transitions between disease states are governed by probability of
381 vaccination (ν, 0–80% annually), force of infection (λ, which varies spatially), and weekly
382 infectious probability (δ, which varies with time spent in the exposed state). Agents in the
383 exposed state have a 10% probability of transitioning to the recovered state rather than the
384 infectious state. Demographic processes include birth (b), immigration (i), emigration (e), and
385 death (d; all agents in the infectious state die after 1 week).
386

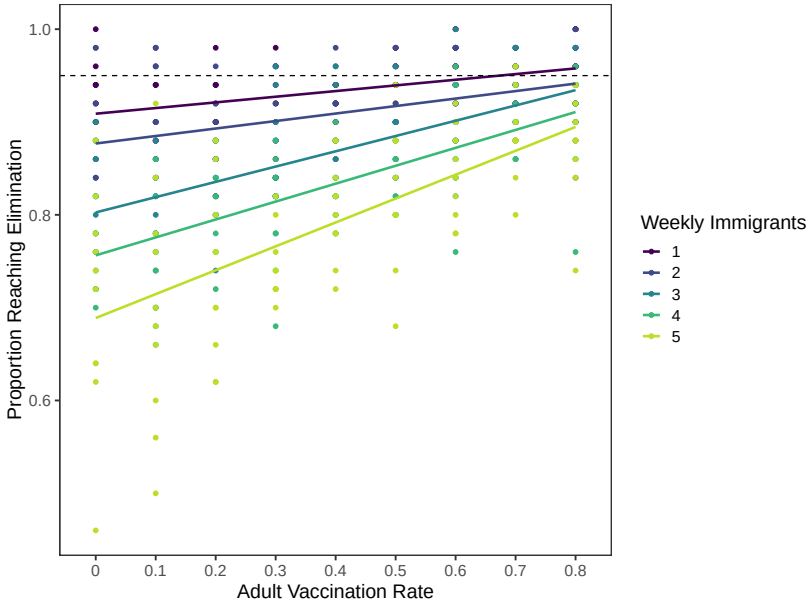

Figure 2. Proportion of simulations in which the initial rabies outbreak was successfully eliminated. Rabies was more likely to be eliminated in simulations in which adult vaccination rates were high and immigration rates, measured in terms of the expected number of weekly immigrants, were low. Simulations with higher adult vaccination rates were also more resistant to increases in immigration rates, as shown by the smaller decrease in elimination probability with higher immigration rates.

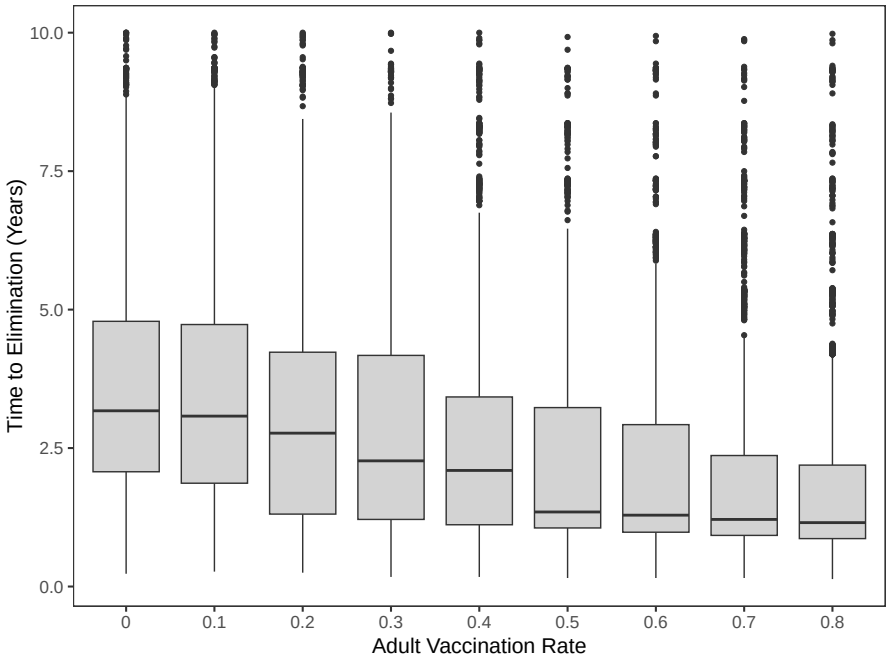

Figure 3. Time to reach rabies elimination (in years) in simulations where rabies was successfully eliminated at least once. Simulations with higher adult vaccination rates generally reached elimination more quickly: simulations with adult vaccination rates of 50% or higher had a median elimination time of less than 1.5 years; whereas simulations with vaccination rates of 0–10% had a median elimination time of greater than 3 years.

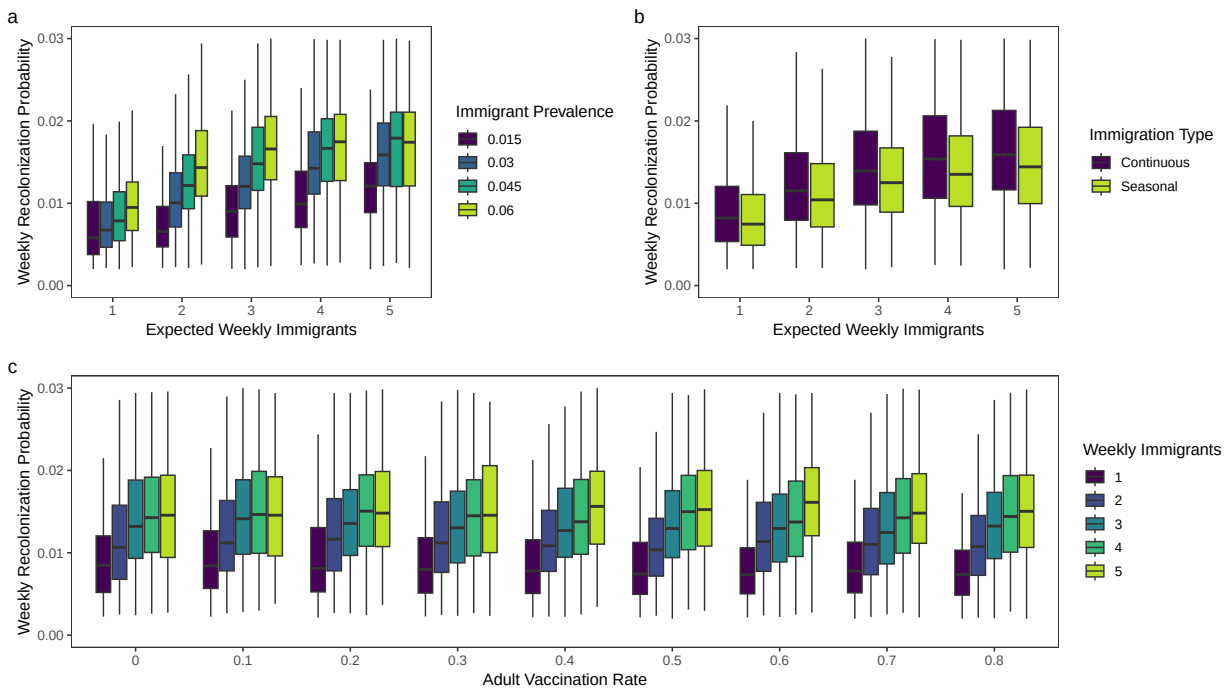

403 **Figure 4.** All immigration variables influenced the weekly probability of rabies recolonization
404 after the initial rabies elimination. Recolonization probability increased with immigration rate
405 (a,b), defined as the expected number of weekly immigrants, and rabies prevalence of
406 immigrants (a). Recolonization was also more likely when immigration occurred continuously
407 rather than seasonally (b). Vaccination rates had no clear effect on recolonization probability (c).
408 Outliers removed for clarity.

Appendix 1: Expanded Methodology and Model Specifications

E.M. Beasley and T. Poisot

The model description herein follows the ODD (Overview, Design concepts, Details) protocol for describing individual-based models, including agent-based models (Grimm et al., 2006, 2010).

Overview

I. *Purpose.*

We used this agent-based model to describe the effects of vaccine-induced immunity and immigration on rabies dynamics in a simulated urban-suburban landscape. Although immigration is likely responsible for the recent re-emergence of rabies cases in Chittenden County, Vermont, data on immigration and emigration in urban areas is sparse and the effects of these processes on rabies dynamics is poorly understood. Because of the relative scarcity of work investigating the role of immigration in sustaining and re-establishing rabies in urban areas, we used this model to provide a baseline understanding of these processes. We designed the model to be flexible enough to incorporate more complex scenarios, such as variability in individual habitat selection behavior or more realistic vaccination scenarios.

II. *Entities, state variables, and scales*

The model consisted of two entities: agents and grid cells. Each grid cell represented a 0.5 x 0.5 km^2 section of the landscape and contained the attributes habitat type (e.g. forest, low

urban development, pasture, etc.) and a vaccination probability for agents over 52 weeks of age. Each agent represented a raccoon and has a variety of attributes (Table 1-1).

Table 1-1. Attributes of simulated agents.

Attribute	Description
ID	Unique identifier for each agent
Position	Coordinates of agent at time step *t*
Home Range Attractor	Coordinates of the agent's home range attractor
Incubation	Binary indicator of the agent's disease state. 0 = uninfected, 1 = infected with rabies
Time since infection	If incubation = 1, the number of weeks since the agent entered the incubation state
Contagious	If incubation = 1, binary indicator of the agent's contagious state. 0 = not contagious (i.e. cannot spread disease), 1 = contagious
Time since contagious	If contagious = 1, the number of weeks since the agent entered the contagious state
Sex	Sex of each agent; 0 = male, 1 = female
Mother	ID of the agent's mother
Immunity	Binary indicator of an agent's immunity status, 0 = not immune to disease, 1 = immune to disease
Age	Age of the agent in weeks

The model landscape consisted of a 60 x 60 square grid, for a total simulation area of approximately 30 km^2. The boundaries of the landscape were reflective, i.e. agents generally could not leave the landscape (see the dispersal submodel in section VII: Submodels for exceptions). Each time step represented 1 week and simulations were run for 11 years, with 52 time steps per year.

III. *Process overview and scheduling*

Time in the simulations was modeled as discrete 1-week steps. Grid cell attributes were fixed for the duration of each simulation, but agent attributes could be changed weekly, or during particular time steps within each year (i.e. seasonally). The first year of the 11-year simulation was treated as a burn-in period to allow the agent population to stabilize before the disease was introduced (i.e. a unique event). The full model schedule can be found in Table 1-2.

Table 1-2. Scheduling of model processes. Within frequency categories, processes are presented in the order in which they occur. Immigration timing varied depending on the simulated scenario and either occurred weekly (consistent immigration) or seasonally.

Frequency	Time step	Event	Description
Weekly		Mortality	Agents are removed from the simulation due to stochastic, old age, disease-induced, and carrying capacity-induced mortality
		Movement	Agents' weekly positions are updated
		Disease transmission	Contagious agents can infect new agents
		Immigration (consistent)	New agents over 52 weeks of age which are not associated with any existing agents are added to the simulation
		Disease state change	Agents which are infected can become contagious or can shed the infection and immune. Time since infection and time since contagious attributes increase by 1
Seasonally	Week 18	Reproduction	New agents with age 0 that are associated with existing female agents are added to the simulation
	Week 35	Vaccination	Agents which are not immune can become immune
	Week 43	Dispersal	Agents' home range attractor can be updated; if the new home range attractor is outside of the landscape boundary, the agent is removed from the simulation

	Week 40-50	Immigration (seasonal)	New agents over 52 weeks of age which are not associated with any existing agents are added to the simulation
Unique	Year 2, Week 1	Disease initialized	10 agents are randomly selected from non-immune agents and become infected

452

453 **Design Concepts**

454 IV. *Design Concepts*

455 *Basic Principles.* We designed our agent-based model as a spatially explicit SEIR model,
456 with additional demographic processes such as births, deaths, immigration, and emigration
457 (Figure 1-1). The spatially explicit component of the model primarily affects the force of
458 infection parameter λ, which varies based on the proximity of an agent to a contagious agent
459 (Figure 1-2). The spatially explicit component of the model also influences the demographic
460 parameters *e* (emigration) and *d* (death) due to increased mortality rates and increased
461 probability of dispersal (therefore increasing the likelihood of an agent leaving the landscape) in
462 grid cells in which the number of agents exceeds the carrying capacity.

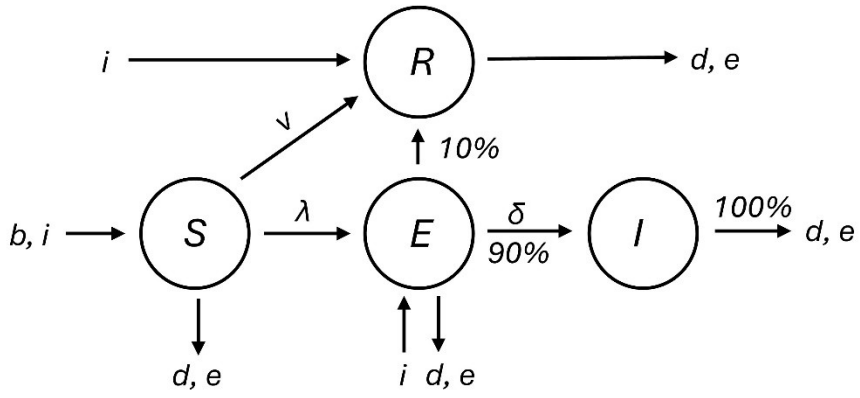

463

464 **Figure 1-1.** Transitions between susceptible (S), exposed (E), infected (I), and recovered (R)
465 disease states of the model. Transitions between disease states are governed by probability of
466 vaccination (*v*, 0–80% annually), force of infection (λ, which varies spatially), and weekly

infectious probability (δ, which varies with time spent in the exposed state). Approximately 90% of exposed individuals eventually transition to the infectious state; approximately 10% instead transition to the recovered state. Demographic processes include birth (b), immigration (i), emigration (e), and death (d; all agents in the infectious state die after 1 week).

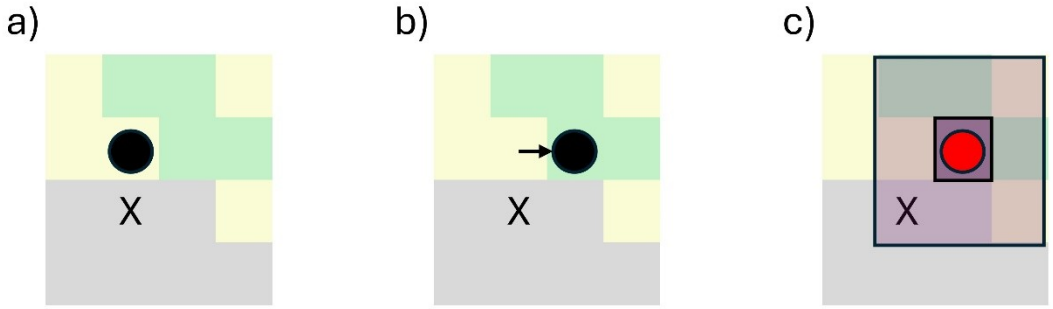

Figure 1-2. a) Each agent in the model is assigned a home range attractor (black X), which can change during the annual dispersal period, and a position (black circle), which can change each week. The agent's weekly position (b) is selected from the previous position's Moore (9-cell) neighborhood, with the probability of selection weighted based on the habitat type, distance from the home range attractor, and the number of agents in each of the possible target cells. If the agent is in the infectious period of the disease (c, red circle), it can infect agents within 500 m of its current position with a probability λ_1. Agents within 1 km of the infected agent's position are infected with a lower probability λ_2.

The disease and demographic processes are heavily influenced by the movement of individual agents in the simulation landscape. Movements can be categorized into two types: weekly and seasonal movements. Weekly movements result in changes in an agent's weekly position in the landscape and are influenced by the habitat type, number of agents, and distance

from the agent's home range attractor of each grid cell in the agent's Moore (9-cell) neighborhood. Agents can also disperse seasonally (i.e. update the location of their home range attractor). Agents less than 52 weeks of age always undergo the dispersal process; however, their dispersal distance can be 0, effectively representing an agent that does not disperse from its natal home range. Agents over 52 weeks of age can disperse if the number of agents in the agent's current cell exceeds the cell's carrying capacity. Similarly to agents less than 52 weeks of age, the dispersal distance can be 0. For more details, see the movement submodel in Section VII: Submodels.

Interactions. Direct interactions between agents influence disease transmission and agent movement. For weekly agent movement, an agent's weekly position is influenced by the number of agents in a given cell within movement range, among other factors. Agents less than 20 weeks of age always inhabit the same cell as their mother. On a seasonal basis, agents over 52 weeks of age can disperse if the number of agents in their current position exceeds the carrying capacity of that cell. Interactions between agents are also assumed, but not explicitly defined, in the disease transmission submodel. A contagious agent can transmit the disease to agents within 500 m of the infectious agent's position with a given probability λ_1, and can transmit the disease to agents within 1 km of the agent's current position with a probability λ_2 (Figure 1-2). These values were chosen based on the results of a parameter sensitivity analysis (Appendix 2). In both cases, it assumed that the contagious agent must have contact with another agent in order to spread the disease, given that rabies is transmitted via direct contact. See the disease transmission submodel in Section VII: Submodels for more details.

Stochasticity. Most processes in the model are at least partially stochastic. The biological realities these processes represent are often highly variable, and the causes of this variability are

not always understood. We are more interested in exploring the consequences of this variability rather than its causes: e.g., we are interested in how varying immigration rates influence rabies persistence, but not necessarily in the biological causes leading to changes in immigration rates. Therefore, we have used stochasticity to generate variability in parameter values and processes that roughly matches the variability observed in real systems. For specific information on how stochasticity is implemented in specific processes, see Section VII: Submodels.

Details

V. *Initialization*

Landscape initialization. We initialized the 60 x 60 landscape using the midpoint displacement algorithm in the Neutral Landscapes package in Julia (Etherington et al., 2015; Fournier et al., 1982). We supplied an autocorrelation parameter that matches the landscape autocorrelation of the greater Burlington, Vermont, area; upon which our simulations are loosely based (see Section VI: Inputs for details). We then reclassified the landscape into discrete habitat categories, the relative proportions of which matched the land cover composition of Burlington. We then created a 5-cell zone of a unique "buffer" habitat on the outer sides of the simulated landscape. The purpose of the buffer is twofold: 1) to reduce the effects of artificial boundaries in the simulated landscape (see the movement submodel in Section VII: Submodels) and 2) to represent the rural landscape surrounding the greater Burlington area, which differs in raccoon density, movement patterns, and vaccine-induced immunity rates (Bastille-Rousseau et al., 2024; Fehlner-Gardiner et al., 2012; Prange et al., 2004).

Initializing agents. We populated non-buffer cells of the simulated landscape using a Poisson point process in which the expected number of agents per cell (λ) was 1.5. All disease-

related attributes were set to 0 (i.e. no agent had contracted the disease). Agent sex and age were stochastically assigned: each agent had a 50% probability of being male or female, whereas each agent's age in weeks was randomly selected from a range of 52–416 weeks (the maximum age in the simulation). Immunity status was assigned as the outcome of a Bernoulli trial, in which the probability of an agent being immunized varied based on the user-defined vaccination probability. Buffer cells were populated using the same procedure, but with a lower expected number of agents per cell ($\lambda = 1$) and a fixed probability of disease immunity (0.6). The initial vaccination probability in the buffer zone is based on the USDA's target vaccine-induced immunity rates, which is frequently achieved in rural areas (Fehlner-Gardiner et al., 2012; Johnson et al., 2021).

VI. *Inputs*

We simulated landscapes based on NLCD land cover data from the greater Burlington, Vermont area (Homer et al., 2015). We obtained land cover at a 30m x 30m resolution from the NLCD website and trimmed the raster to an extent of -73.347 – -73.0.17 degrees longitude and 44.374 – 44.587 degrees latitude. We reclassified the land cover data based on land cover categories used in the National Rabies Management Program Oral Rabies Vaccine baiting algorithm (McClure et al., 2022). After land cover reclassification, we calculated 1) the proportion of each land cover type in the landscape and 2) a spatial autocorrelation index using the function `lsm_l_ai` in the R package `landscapemetrics` (Hesselbarth et al., 2019). The land cover proportions and autocorrelation index were used to generate simulated landscapes.

VII. *Submodels*

The following submodels are presented in the order in which they occur in the simulation.

Mortality. There were several sources of mortality, in which agents were removed from the landscape. Each week, agents could be stochastically removed from the landscape with a probability of 0.001, which represented all potential sources of mortality that were not explicitly defined here (e.g., vehicle collisions). All agents in the contagious state of the disease died after having been in the contagious state for 2 weeks. Because disease mortality occurs before disease transmission in each time step, this corresponds to 1 week in which the agent can potentially spread the disease to other agents. Agents were removed from the simulation upon reaching 416 weeks (8 years) of age. Finally, agents with a weekly position in a cell that exceeded carrying capacity were subjected to higher weekly mortality rates: agents at least 52 weeks of age had a carrying capacity mortality rate of 0.005, whereas agents younger than 52 weeks of age had a carrying capacity mortality rate of 0.02. These differential mortality rates lead to increased mortality among younger agents, which is observed in real populations (Pitt et al., 2008).

Movement. Each agent in the simulation can potentially update their weekly position. For agents at least 20 weeks of age (i.e. agents old enough to move independently of their mother), each agent selected a position from within the current cell's 9-cell (Moore) neighborhood, which includes the agent's current position and the eight adjacent landscape cells. These cells were selected using a weighted probability that accounted for 1) the habitat type in each cell, 2) the distance from the agent's home range attractor, and 3) the number of agents occupying each cell in the previous time step. We weighted each component process independently, then calculated

577 the final weight as a product of the three processes. Weighted probabilities were calculated using
578 the `Weights` function in the StatsBase package in Julia v. 1.9.2 (Bezanson et al., 2017).

579 To account for habitat type in each agent's weekly movement, we used resource selection
580 function (RSF) coefficients calculated by McClure et al. (2022) as the values for each weighted
581 probability calculation. We used population-level coefficients rather than individual-level
582 coefficients to calculate movement probabilities: a decision which omits the individual
583 variability found in real populations, which may in turn influence disease dynamics. However,
584 reducing individual variability in movement reduces some of the "noise" from this variability,
585 allowing us to focus on the effects of immigration and population-level immunity. We accounted
586 for distance from an agent's home range attractor using methods derived from Signer et al.
587 (2017) (Eq. 1-1):

588 $$p(c_{t+1}) \propto \exp(-\omega\, d(c_{t+1})) \qquad \text{(Eq. 1-1)}$$

589 In which $p(c_t)$ the probability of a raccoon occupying cell c within the raccoon's current Moore
590 neighborhood at time $t+1$, ω the strength of attraction towards the location of the home range
591 attractor, and $d(c_t)$ the squared distance between potential target cells and the home cell. The
592 squared distance between cells was calculated by (Eq. 1-2):

593 $$d(c_t) = \frac{r\left((x_t - x_h)^2 + (y_t - y_h)^2\right)}{100} \qquad \text{(Eq. 1-2)}$$

594 After agents at least 20 weeks old selected their weekly position, the position of any
595 agents less than 20 weeks old was updated to match their mother's.

596 *Disease transmission.* Only agents in the infectious state of the disease could transmit the
597 disease (Figure 1-1). Furthermore, these agents could only transmit the disease to agents within 1
598 km of their current weekly position which had not acquired immunity through vaccination or
599 recovery from the exposed state. Disease transmission had a spatial component (Figure 1-2) in

600 which agents had a higher probability of transmitting the disease to agents within 500 m of their
601 current position (λ_1) than to agents within 1 km of their current position (λ_2). These probabilities
602 were selected using a parameter sensitivity analysis (Appendix 2). Although it is more common
603 to use a continuous distance-decay function to account for spatial effects on disease transmission,
604 the grain size of the simulation (0.5 x 0.5 km) compared to the typical weekly home range size of
605 raccoons in urban-suburban landscapes such as Burlington (mean radius 600m, McClure et al.,
606 2022) would essentially result in discrete transmission probabilities. We supplied these
607 probabilities based on the results of a parameter sensitivity analysis rather than calculating them
608 each time step to reduce computation time.

609 *Change disease state.* Each week, an agent in the exposed state of the disease could
610 recover from the disease with a probability of 0.002. Recovered agents obtained lifelong
611 immunity to the disease. Agents which did not recover transitioned to the infectious state with a
612 probability drawn from a beta distribution $P \sim Beta(t, 5)$, in which t is the number of weeks since
613 the agent was exposed to the disease. These weekly probabilities resulted in a total probability of
614 recovery of 8–12% and a typical disease incubation period of 4–6 weeks, which is consistent
615 with observed values (see Appendix 2 for details).

616 *Update temporal attributes.* Each agent's age, time since infection (if in the exposed
617 state), and time since entering the infectious state (if in the infectious state) was increased by 1
618 each week.

619 *Immigration.* Immigration could occur either weekly (consistent immigration) or
620 seasonally. When immigration was set to be consistent, the number of immigrants per week was
621 drawn from a Poisson distribution $N \sim Pois(n)$, in which n took values of 1–5 expected
622 immigrants per week. Most immigrant attributes were assigned the same way as the initial

623 population (see Section V: Initialization); with the exception of the agents' position, immunity
624 status, and incubation status. Each agent immigrating into the landscape was assigned an initial
625 position along one of the edges of the simulated landscape. Each immigrating agent could be
626 incubating the disease with a user-defined probability which could take values of 0, 0.015, 0.03,
627 0.045, and 0.06. All immigrants were assumed to have an immunity status of 0. After attributes
628 were assigned, immigrants were randomly assigned a movement direction that would not
629 immediately take them out of the simulated landscape, and a movement distance. Agents then
630 moved to a new position based on these parameters.
631 Seasonal immigration took place between weeks 40 and 50 of the simulation. The
632 procedure is the same as consistent immigration, with the exception that the number of weekly
633 immigrants was determined by $N \sim Pois(n*5)$, which resulted in approximately the same total
634 number of immigrants for the duration of each simulation (Appendix 2).
635 *Reproduction.* Reproduction occurred at week 18 of each year in the simulation. Female
636 agents were randomly selected to reproduce with a probability of 95% (Rees et al., 2013; Tinline
637 et al., 2007). We then assigned the number of offspring for each reproducing female by drawing
638 from a Poisson distribution $N_i \sim Pois(4)$, in which N_i was the number of offspring produced by
639 agent i. With this distribution a litter size of 0 was possible, but rare. Each offspring was assigned
640 a value of male or female with a 50% probability and its initial position was the same as the
641 mother's. Offspring were also assigned a unique identifier and all disease and vaccination states
642 were set at 0. Although it is likely that immune female raccoons confer some rabies immunity to
643 their offspring, we did not incorporate this into the model because the duration and strength of
644 rabies resistance conferred this way is currently unknown (Fry et al., 2013).

Vaccination. Vaccination success of a given agent during the annual vaccination period (week 35) was based on the agent's age and position. Agents in the buffer zone which were at least 1 year old had a vaccination probability of 60%, consistent with empirical vaccination rates in rural areas (Fehlner-Gardiner et al., 2012). Agents elsewhere in the landscape that were at least 1 year old were vaccinated with a user-defined probability that ranged from 0–80% at 10% intervals. Agents less than 1 year old had a vaccination probability that was half of the probability for agents older than 1 year (Beasley et al., 2024).

Dispersal. Seasonal dispersal as defined here includes a potential change in 1) the agent's current position and 2) the location of an agent's home range attractor. The dispersal function was activated in week 43 of each year of the simulation and was largely the same for raccoons of all ages. Starting from the agent's current position, each agent undergoing dispersal was assigned a movement direction and distance. Movement direction was defined by randomly selecting one of the eight cells in the agent's Moore neighborhood (Cullingham et al., 2008). Movement distance was defined as the number of landscape cells traveled and was drawn from a Poisson distribution with an expected movement distance λ that varied based on the agent's age (it was possible for any agent to have a movement distance of 0). The agents then moved to a new position according to their assigned movement distance and direction. Agents whose updated position fell outside of the landscape boundary were permanently deleted from the simulation. All other agents' home range attractor was updated to the agents' new position. This process was repeated until the agent reached a grid cell below carrying capacity or until 3 movements were made, whichever occurred first.

Although the overall dispersal process was the same for raccoons of all ages, there were slight differences between agents less than one year of age and all other agents. All agents less

than one year old were subject to the dispersal process, whereas agents at least one year old only went through the dispersal process if they were occupying a cell above carrying capacity. The expected movement distance also varied based on age: the expected distance for agents less than 1 year of age was 3 grid cells (1.5 km), other agents had an expected distance of 2 grid cells (1 km). These distances are consistent with empirical dispersal distances (Rees et al., 2008).

Disease initialization. We initialized the disease in week 1 of year 2 by randomly selecting 10 non-immune agents and changing their incubation state to 1.

Additional Literature Cited

Bastille-Rousseau, G., Gorman, N. T., McClure, K. M., Nituch, L., Buchanan, T., Chipman, R. B., Gilbert, A. T., & Pepin, K. M. (2024). Assessing the Efficiency of Local Rabies Vaccination Strategies for Raccoons (Procyon lotor) in an Urban Setting. *Journal of Wildlife Diseases*, *60*(1). https://doi.org/10.7589/JWD-D-23-00059

Beasley, E. M., Nelson, K. M., Slate, D., Gilbert, A. T., Pogmore, F. E., Chipman, R. B., & Davis, A. J. (2024). Oral Rabies Vaccination of Raccoons (Procyon lotor) across a Development Intensity Gradient in Burlington, Vermont, USA, 2015–2017. *Journal of Wildlife Diseases*, *60*(1), 1–13. https://doi.org/10.7589/JWD-D-22-00117

Bezanson, J., Edelman, A., Karpinski, S., & Shah, V. B. (2017). Julia: A fresh approach to numerical computing. *SIAM Review*, *59*(1), 65–98.

Cullingham, C. I., Pond, B. A., Kyle, C. J., Rees, E. E., Rosatte, R. C., & White, B. N. (2008). Combining direct and indirect genetic methods to estimate dispersal for informing wildlife disease management decisions. *Molecular Ecology*, *17*(22), 4874–4886. https://doi.org/10.1111/j.1365-294X.2008.03956.x

Etherington, T. R., Holland, E. P., & O'Sullivan, D. (2015). NLMpy: A python software package for the creation of neutral landscape models within a general numerical framework.

Methods in Ecology and Evolution, *6*(2), 164–168. https://doi.org/10.1111/2041-210X.12308

Fehlner-Gardiner, C., Rudd, R., Donovan, D., Slate, D., Kempf, L., & Badcock, J. (2012). Comparing ONRAB And RABORAL V-RG oral rabies vaccine field performance in raccoons and striped skunks, New Brunswick, Canada, and Maine, USA. *Journal of Wildlife Diseases*, *48*(1), 157–167.

Fournier, A., Fussell, D., & Carpenter, L. (1982). Computer rendering of stochastic models. *Communications of the ACM*, *25*(6), 371–384. https://doi.org/10.1145/358523.358553

Fry, T. L., VanDalen, K. K., Shriner, S. A., Moore, S. M., Hanlon, C. A., & VerCauteren, K. C. (2013). Humoral immune response to oral rabies vaccination in raccoon kits: Problems and implications. *Vaccine*, *31*(26), 2811–2815. https://doi.org/10.1016/j.vaccine.2013.04.016

Grimm, V., Berger, U., Bastiansen, F., Eliassen, S., Ginot, V., Giske, J., Goss-Custard, J., Grand, T., Heinz, S. K., Huse, G., Huth, A., Jepsen, J. U., Jørgensen, C., Mooij, W. M., Müller, B., Pe'er, G., Piou, C., Railsback, S. F., Robbins, A. M., … DeAngelis, D. L. (2006). A standard protocol for describing individual-based and agent-based models. *Ecological Modelling*, *198*(1), 115–126. https://doi.org/10.1016/j.ecolmodel.2006.04.023

Grimm, V., Berger, U., DeAngelis, D. L., Polhill, J. G., Giske, J., & Railsback, S. F. (2010). The ODD protocol: A review and first update. *Ecological Modelling*, *221*(23), 2760–2768. https://doi.org/10.1016/j.ecolmodel.2010.08.019

Hesselbarth, M. H. K., Sciaini, M., With, K. A., Wiegand, K., & Nowosad, J. (2019). landscapemetrics: An open-source R tool to calculate landscape metrics. *Ecography*, *42*(10), 1648–1657. https://doi.org/10.1111/ecog.04617

Homer, C., Dewitz, J., Yang, L., Jin, S., Danielson, P., Xian, G., Coulston, J., Herold, N., Wickham, J., & Megown, K. (2015). Completion of the 2011 National Land Cover Database for the Conterminous United States – Representing a Decade of Land Cover

Change Information. *Photogrammetric Engineering & Remote Sensing*, *81*(5), 345–354. https://doi.org/10.1016/S0099-1112(15)30100-2

Johnson, S. R., Slate, D., Nelson, K. M., Davis, A. J., Mills, S. A., Forbes, J. T., VerCauteren, K. C., Gilbert, A. T., & Chipman, R. B. (2021). Serological responses of raccoons and striped skunks to Ontario rabies vaccine bait in West Virginia during 2012–2016. *Viruses*, *13*(2), 157.

McClure, K. M., Bastille-Rousseau, G., Davis, A. J., Stengel, C. A., Nelson, K. M., Chipman, R. B., Wittemyer, G., Abdo, Z., Gilbert, A. T., & Pepin, K. M. (2022). Accounting for animal movement improves vaccination strategies against wildlife disease in heterogeneous landscapes. *Ecological Applications*, *32*(4), e2568.

Pitt, J. A., Larivière, S., & Messier, F. (2008). Survival and Body Condition of Raccoons at the Edge of the Range. *The Journal of Wildlife Management*, *72*(2), 389–395. https://doi.org/10.2193/2005-761

Prange, S., Gehrt, S. D., & Wiggers, E. P. (2004). Influences of anthropogenic resources on raccoon (Procyon lotor) movements and spatial distribution. *Journal of Mammalogy*, *85*(3), 483–490.

Rees, E. E., Pond, B. A., Phillips, J. R., & Murray, D. (2008). Raccoon ecology database: A resource for population dynamics modelling and meta-analysis. *Ecological Informatics*, *3*(1), 87–96. https://doi.org/10.1016/j.ecoinf.2008.01.002

Rees, E. E., Pond, B. A., Tinline, R. R., & Bélanger, D. (2013). Modelling the effect of landscape heterogeneity on the efficacy of vaccination for wildlife infectious disease control. *Journal of Applied Ecology*, *50*(4), 881–891. https://doi.org/10.1111/1365-2664.12101

Signer, J., Fieberg, J., & Avgar, T. (2017). Estimating utilization distributions from fitted step-selection functions. *Ecosphere*, *8*(4), e01771. https://doi.org/10.1002/ecs2.1771

Tinline, R., Ball, D., Broadfoot, J., & Pond, B. (2007). The Ontario rabies model. *Queens University, Kingston, Ontario, Canada*.

Appendix 2: Model Functionality Testing and Parameter Sensitivity Analysis

E.M. Beasley and T. Poisot

We tested various aspects of the agent-based model (see Appendix 1 for detailed descriptions of individual functions) to ensure they were producing expected outputs. For most model parameters, we assigned values based on empirical data, but for parameters for which empirical values were limited, we conducted a parameter sensitivity analysis to identify values that produced realistic outcomes. Results of both tests are discussed below. Unless otherwise indicated, functionality tests and parameter sensitivity analyses were completed without agents immigrating into the landscape.

Functionality Tests

Cell Size

We chose a 0.5 x 0.5 km cell for our spatial grain size. This grain size reduces computational intensity compared to a smaller grain size (e.g. the 30 x 30 m resolution of the available land cover data). Additionally, there is little habitat heterogeneity at the 30 x 30 m resolution in the greater Burlington area, the empirical landscape from which we derived the characteristics of our simulated landscapes. As a result, the autocorrelation of the original 30 x 30 m landscape calculated using the package `landscapemetrics` (Hesselbarth et al., 2019) was similar to the landscape with a 0.5 x 0.5 km resolution (75.8 vs. 77.4, respectively). The major features in a map of Burlington at a 30 x 30 m resolution were still present in a map with a 0.5 x 0.5 km resolution (Figure 2-1).

We decided against using a larger grain size than 0.5 x 0.5 km because 1) the major landscape features are less identifiable at larger grain sizes, and 2) increasing the grain size would restrict agents' home ranges to approximately 1 cell or less, which would prevent agents from readily changing their weekly position.

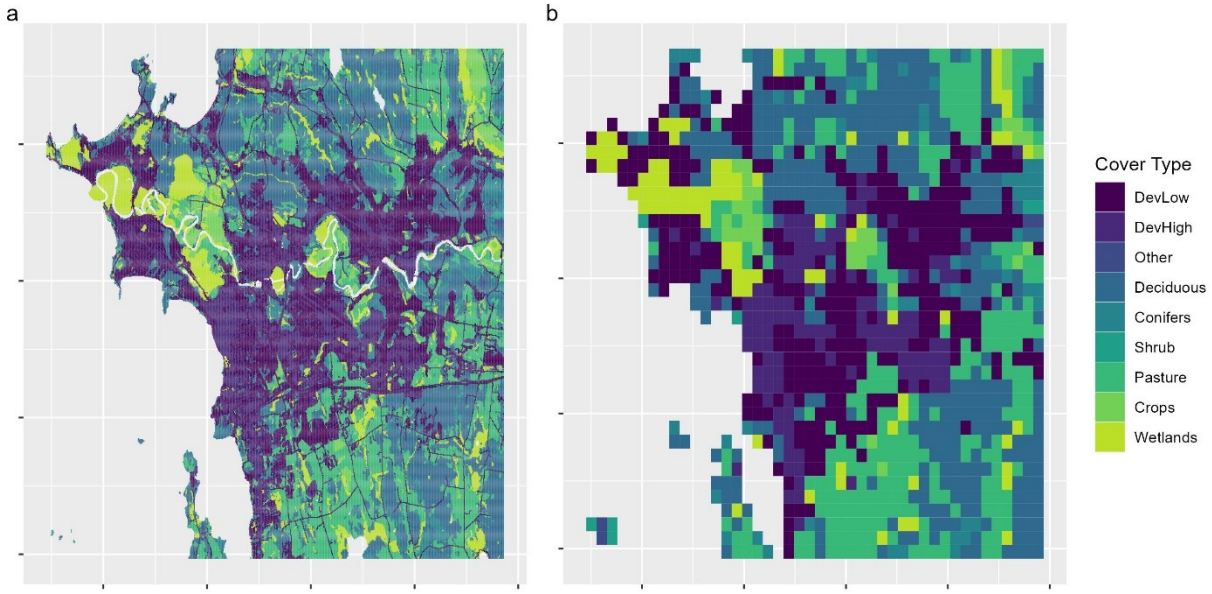

Figure 2-1. Map of the greater Burlington, VT area at a 30 x 30 m resolution (a) and 0.5 x 0.5 km resolution (b). Due to a high degree of spatial autocorrelation in land cover, major landmarks, including the wetlands of the Winooski River delta and Intervale Center farmland in the top-left corner, and the municipalities of Burlington, South Burlington, Winooski, and Essex Junction in the center, are still recognizable with the larger spatial grain.

Landscape Generation Algorithm

We used the midpoint displacement algorithm in the Julia package `NeutralLandscapes` (Poisot et al., 2023), which is a port of the Python package `NLMpy`

(Etherington et al., 2015), to generate our simulated landscapes. This algorithm simulates a landscape of values of a continuous variable such as elevation, the autocorrelation of which is specified by the user (Fournier et al., 1982; Palmer, 1992). We calculated the spatial autocorrelation of Burlington habitat data using `lsm_l_ai` function in the R package `landscapemetrics` (Hesselbarth et al., 2019) and used that value in the mid-point displacement algorithm. After generating a continuous landscape using the mid-point displacement algorithm, we re-classified the simulated landscape into discrete categories based on the relative proportions of available habitat in Burlington (Figure 2-2). We also placed a unique "buffer" habitat on the outermost 5 cells on each side of the simulated landscape, which were used to reduce boundary effects in the simulation (see Appendix 1 for more details).

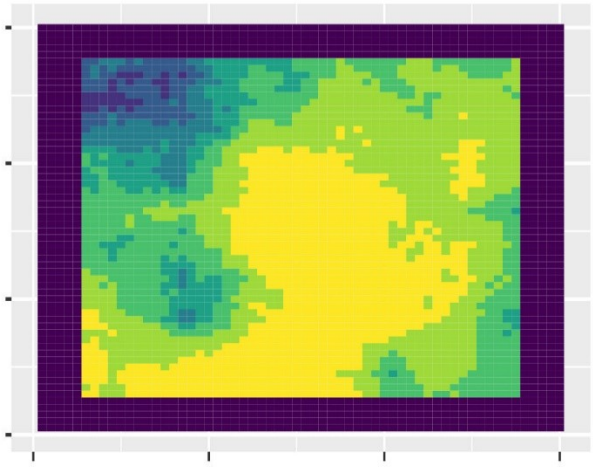

Figure 2-2. Example landscape generated using a mid-point displacement algorithm and re-classified into discrete habitat categories. Spatial autocorrelation and relative proportions of land cover categories were calculated from land cover data of the greater Burlington, VT area.

Weekly Position and Seasonal Home Range

Each agent was assigned a weekly position at each time step in the simulation, which represented the center of the agent's weekly home range. In addition, each agent was assigned a home range attractor that restricted the agent's movement to a particular geographic area. The home range attractor could be updated annually during the dispersal period. The weekly position was updated each week based on a weighted probability that accounted for 1) the habitat type, 2) conspecific density, and 3) distance from the agent's home range attractor in the agent's current weekly position and the 8 cells surrounding its weekly position. For more details, see the *Movement* subsection of Appendix 1, Section VII: Submodels.

We tested the movement of agents prior to the dispersal period of the model to ensure seasonal home range size was consistent with empirical values from Burlington. Because empirical data from Burlington spans from July–September, we calculated agents' seasonal home ranges from the equivalent weeks of the simulation. A distance-decay rate from the home range attractor of -0.001 resulted in seasonal home ranges that ranged from 0.785–5.935 km^2 in size, with a median value of 1.658 km^2. The median home range size was very close to the empirical median (1.626 km^2); however, there was more variability in the empirical data (range 0.283–11.087 km^2, United States Department of Agriculture Animal and Plant Inspection Service [USDA APHIS], Wildlife Services, unpublished data). Variability in home range sizes can affect rabies persistence (McClure et al., 2020), but because we were primarily interested in the affects of immigration on rabies persistence and recolonization, we chose not to introduce additional variability in seasonal home range size.

Disease State Changes

Rabies typically has a latent period of 3–6 weeks, in which an individual has been infected with the virus but is not yet contagious (Tinline et al., 2007). We modeled the weekly probability of an agent moving from the "exposed" (i.e. infected but not contagious) to the "infectious" (i.e. contagious) state as the outcome of a Bernoulli trial, in which the probability of changing states was drawn from a beta distribution $P \sim Beta(n, 5)$, where n is the number of weeks the agent has spent in the exposed state. This resulted in a typical latent period of 3–6 weeks, which is consistent with empirical values (Figure 2-3).

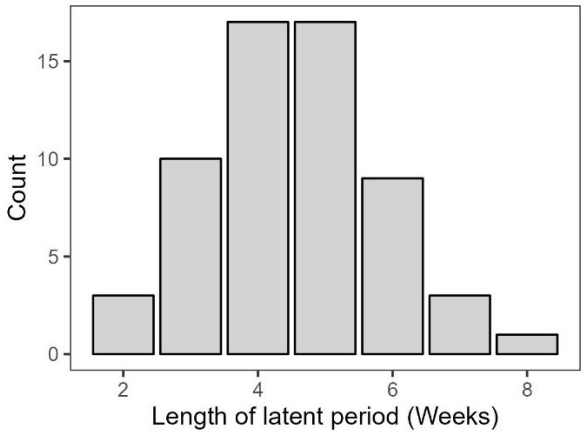

Figure 2-3. Distribution of the length of the latent period of the disease, in weeks. The distribution has a mode of 4–5 weeks; consistent with empirical values.

Raccoons exposed to the rabies virus also have a 10% probability of recovering from the virus rather than becoming infectious (Slate et al., 2014). We modeled the weekly process of an exposed individual entering the recovered state as the outcome of a Bernoulli trial, in which the probability of success was 0.015, resulting in simulated recovery rates ranging from 8–12%.

Parameter Sensitivity Analyses

K_{max} and Carrying Capacity Mortality

Empirical data from Burlington suggests a mean raccoon density of approximately 40/km^2 in July and 30/km^2 in October (Beasley et al., 2024). Density distributions are strongly right-skewed, so total population sizes are likely smaller than these density values would suggest. A max carrying capacity of 40/km^2, an adult density mortality rate of 0.005, and a juvenile density mortality rate of 0.02 typically results in population sizes close to empirical values, with a population that is slowly growing (Figure 2-4).

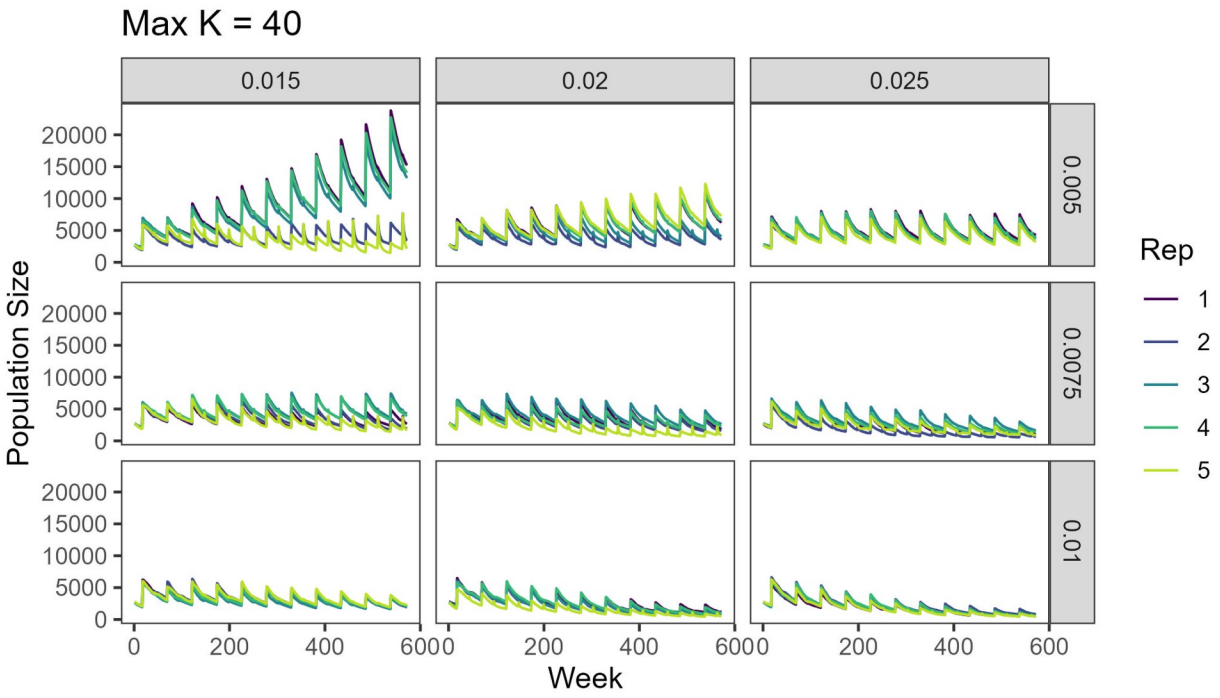

Figure 2-4. Total simulated population sizes across a 10-year simulated period with a maximum carrying capacity *K* set at 40 raccoons/km^2. Population sizes varied according to adult (rows) and juvenile (columns) mortality rates, which occurred when a given cell exceeded the maximum

number of raccoons. At this carrying capacity, an adult mortality rate of 0.005 and a juvenile mortality rate of 0.02 resulted in population sizes that were close to empirical values measured in Burlington in July and October 2015–2017.

We also examined the turnover rate (i.e. births vs. deaths) of the population at the selected carrying capacity and associated mortality rates, because turnover affects the relative proportion of susceptible to recovered/vaccinated individuals in the population. We simulated 2 years of the population: one without the disease, and one following disease introduction on week 1 of year 2. The annual birth pulse approximately doubled the population during the week in which births occurred. However, year-over-year population growth with the density mortality rates described above ranged from -1.58%–1.79%, with a median growth rate of 1.29%.

Weekly deaths ranged from 0.6–7.5% of the population, with a median of 1.4%. Prior to disease introduction, mortality rates were highest between weeks 20 and 40 of the simulation (Figure 2-5) due to high carrying capacity mortality of agents less than 52 weeks of age, which ranged from 20–100% of deaths with a median of 61.5% of deaths during this time period. This is qualitatively consistent with higher juvenile mortality rates in natural populations (Pitt et al., 2008). Over the course of a year, carrying capacity-induced mortality of agents was the most common source of mortality (74.0% of all mortality events before disease introduction).

After the disease was introduced into the population, mortality rates tended to be higher earlier in the year, although this could be an artifact of disease introduction, as mortality rates with and without the disease were similar at the end of the year (Figure 2-5). The most common source of mortality post-disease introduction was still carrying capacity mortality of agents less than 52 weeks of age, accounting for 40.5% of deaths over the course of the year. Disease-

induced mortality accounted for 35.2% of deaths, while carrying capacity mortality of agents over 52 weeks of age accounted for 13.9% of deaths.

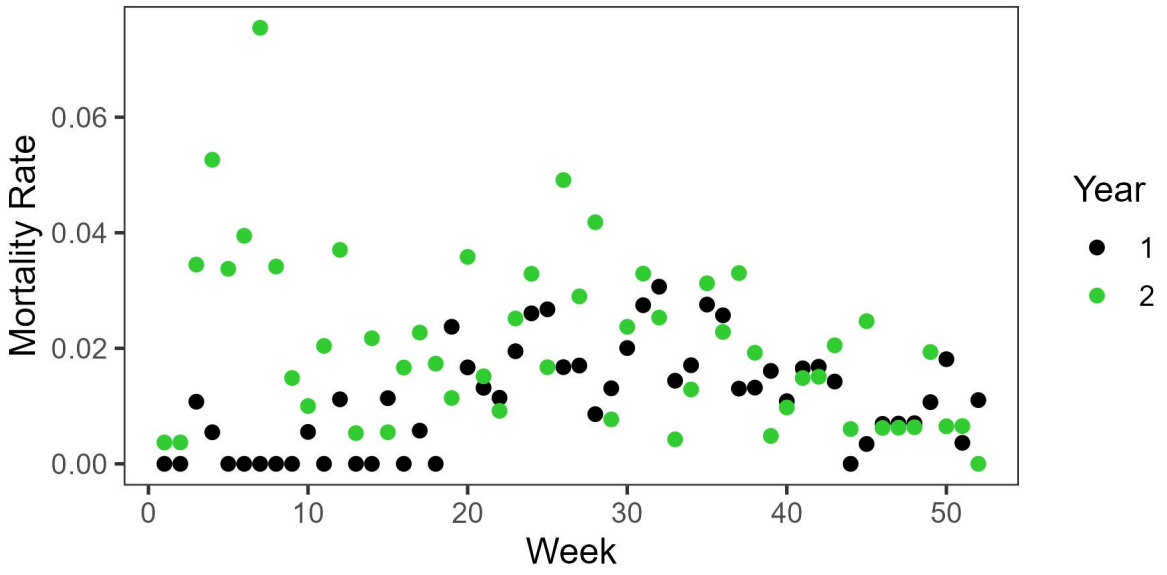

Figure 2-5. Weekly mortality rates before (black) and after (green) rabies was introduced into the simulated population. Mortality rates were generally low, with a median rate of 0.014. Prior to disease introduction, mortality rates were highest between weeks 20 and 40 of the simulation, a time period after the birth of new agents but before the dispersal period. After disease introduction, mortality rates were slightly higher earlier in the year, although this could be an artifact of disease initialization.

Disease Transmission Rates

We tested several combinations of values of core home range (λ_1, corresponding to the transmission rate to raccoons within 500 m of the infectious raccoon) and peripheral home range (λ_2, corresponding to transmission to raccoons within 1 km of the infectious agent) transmission

rates in simulations with the density mortality rates discussed above. We tuned the core home range transmission rate first by performing a wide sweep of parameter values between 0.001 and 0.5 on a logarithmic scale, with 5 replicates per parameter value (Figure 2-6a), and selected a narrower range of parameter values based on the number of weeks needed to reach elimination. We repeated the process on the narrow range values with 10 replicates per parameter. We selected a parameter value for λ_I based on 1) time to elimination, 2) median weekly cases, and 3) the effective reproduction number R_e. A λ_I value close to 0.035 yielded an expected time to elimination of 172 weeks (3.3 years, Figure 2-6b), 5 median weekly cases (Figure 2-7), and an R_0 of approximately 1.32, which were closest to empirical values (Biek et al., 2007; Childs et al., 2000).

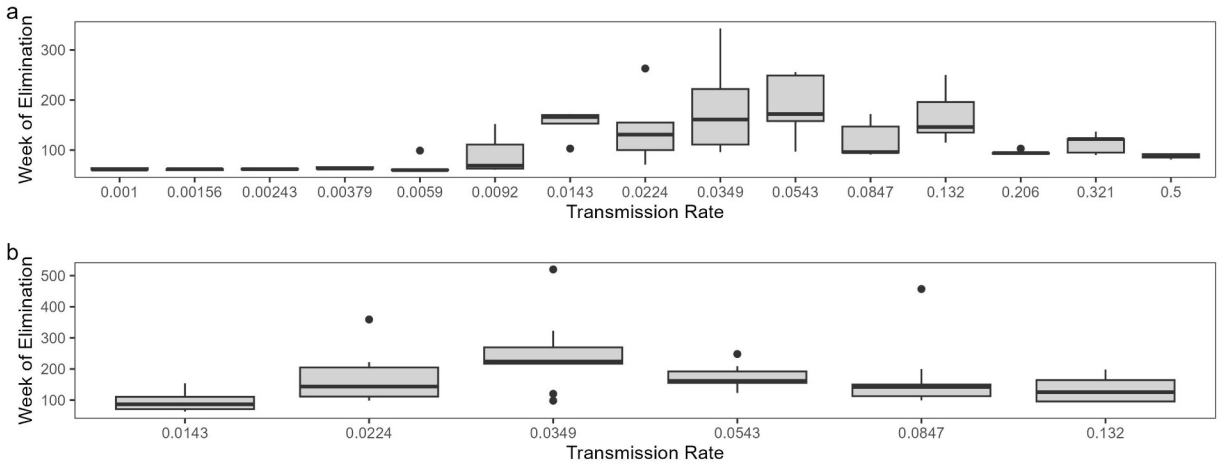

Figure 2-6. Timing of rabies elimination under a variety of transmission rates. A wide parameter sweep with 5 replicates per rate (a) yielded 6 transmission rates in which rabies outbreaks typically lasted more than 2 years. These values were tested again with 10 replicates per rate (b). A transmission rate close to 0.035 yielded a mean elimination time closest to the empirical median of 350 weeks.

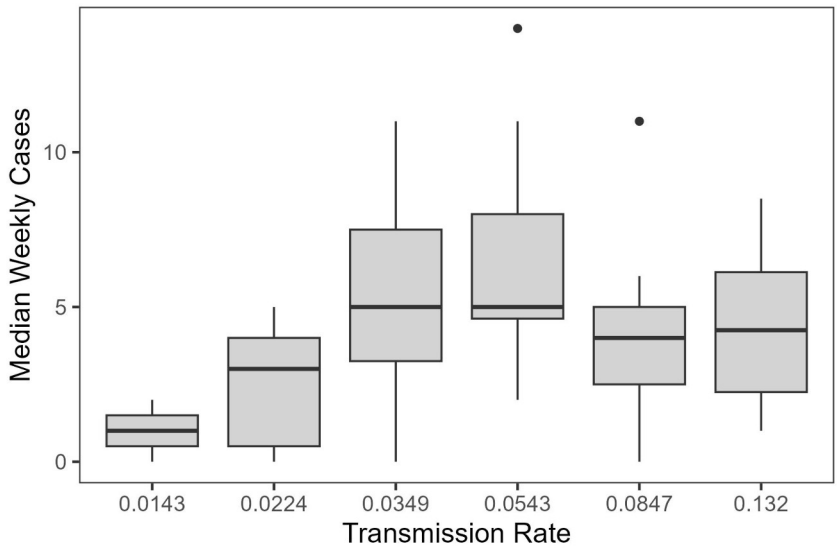

Figure 2-7. Median weekly cases at varying rabies transmission rates in an infected agent's core home range.

We then tested a series of values for transmission rates at the periphery of an infected agent's weekly home range λ_2 (i.e. within 1 km of the agent's current position). We began with a logarithmic sequence of values ranging from 0.001–0.03, with 10 replicates per value and λ_1 fixed at 0.035. We selected values close to 0.03 for further testing because this value resulted in some outbreaks persisting in the landscape (70%), a mean duration of 219 weeks for outbreaks which were eliminated (Figure 2-8), and a median of 2.5 cases per week after the initial outbreak. The estimated R_0 was also 1.22, which is consistent with empirical estimates of R_e (Biek et al., 2007)

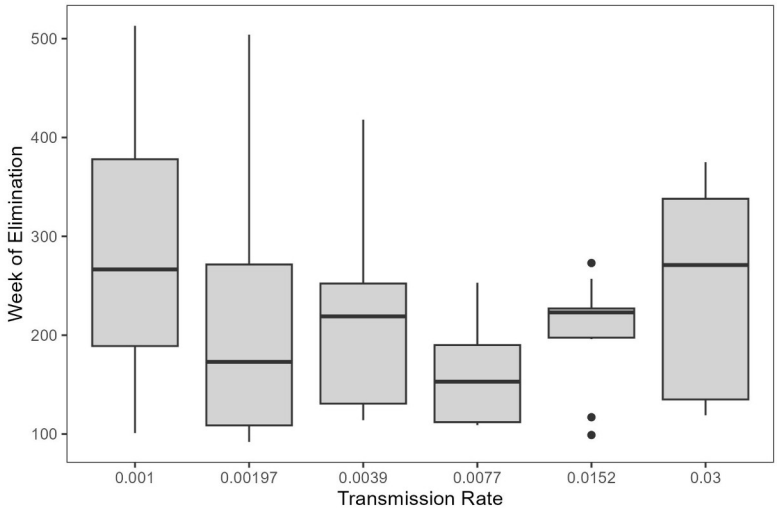

Figure 2-8. Week of elimination for assorted values of λ_2 (i.e. disease transmission in the home range periphery) for simulations in which rabies was eliminated. Values of 0.001 and 0.03 yielded similar elimination timings; however, simulations in which λ_2 was 0.03 were more likely to have rabies persistence over the duration of the simulation.

Lastly, we tested values of λ_2 from 0.1–0.03 at intervals of 0.05, with λ_1 fixed at 0.035. We simulated 20 replicates for each parameter. Of these, we chose a final value of λ_2 of 0.02 due to having the highest probability of persistence (85%) and the most realistic value of R_0 (~1.24). Time to elimination and cases per week were similar among values tested.

We also examined population sizes, as rabies endemicity tends to result in a small but noticeable decrease in population sizes. The initial disease outbreak results in a noticeable decrease in population size, followed by an increase in population as the initial peak in cases subsides (Figure 2-10). This pattern was qualitatively similar across all tested transmission rates.

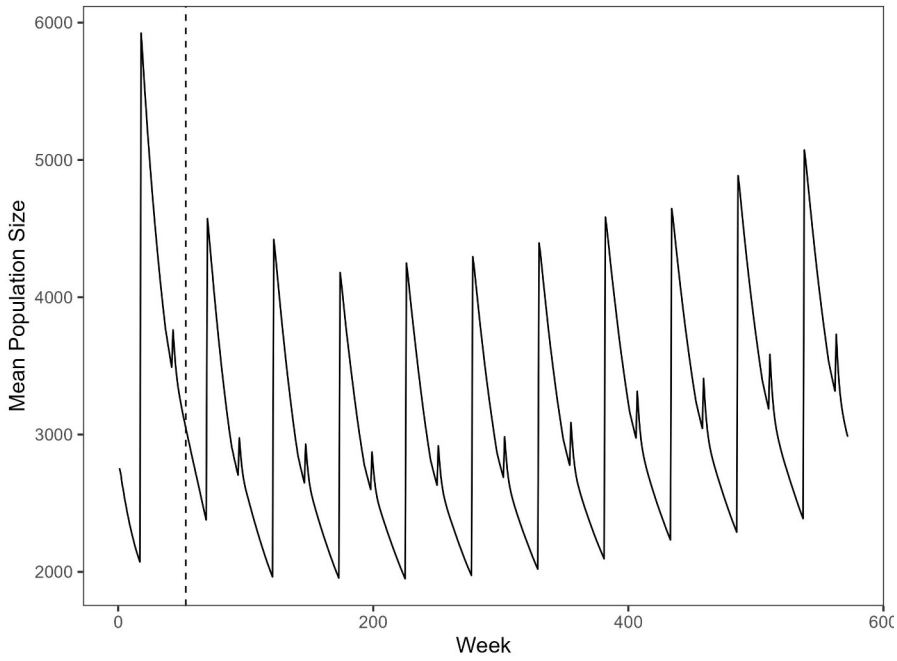

Figure 2-10. Mean population sizes in each week of the simulation with the core home range transmission rate (λ_1) fixed at 0.035 and the peripheral home range transmission rate (λ_2) fixed at 0.02. The simulated population decreases after the disease is introduced into the population (dashed vertical line), but the population then increases to close to the initial size.

Table of Parameters

Values for demographic and epidemiological parameters can be found in the following table (Table 2-1).

Table 2-1. Parameter values for demographic and epidemiological parameters from the agent-based model.

Parameter	Value(s)	Description and Source
Raccoon demographics		
K_{max}	40/km^2	Maximum carrying capacity per cell (Figure 2-5).
Age of independence	20 weeks	Age at which juveniles are no longer maternally dependent: can survive if mother dies & moves independently, but still shares a home range attractor (Rees et al., 2008; Tinline et al., 2007)
Week of birth	Week 18	(Hauver et al., 2010; Rees et al., 2008; Sanderson & Nalbandov, 1973)
Probability of a female > 52 weeks old producing a litter	95%	(Prange et al., 2003)
Litter size	~ Pois(4)	(Rees et al., 2008)
Dispersal timing	Week 43	Adults only disperse if their current position exceeds carrying capacity (Rees et al., 2008)
Dispersal distance	~Pois(3) (< 52 weeks of age) ~Pois(2) (>= 52 weeks of age)	For ~Pois(λ) in which λ represents the number of 0.5 km x 0.5 km grid cells moved (Rees et al., 2008)
Weekly stochastic mortality	0.001	Represents all sources of mortality not explicitly defined here (Gehrt & Prange, 2007; Prange et al., 2003)
Orphan mortality	100%	Applied to raccoons < 20 weeks of age whose mother is dead
Old age mortality	100%	Applied to raccoons over 8 years old (Rees et al., 2013)
Weekly density-related mortality rate	0.005 (>= 52 weeks) 0.02 (< 52 weeks)	Applied to raccoons occupying cells exceeding K_{max} (Figure 2-5)
Immigration Timing	Variable	Immigration occurs weekly (“consistent”) or between weeks 40 and 50 (“seasonal”)
Immigration	~Pois(λ)	Variable. For consistent immigration, λ is set by the user

Rate		(values of 1–5); for seasonal immigration, the number of immigrants is ~Pois(λ*5), resulting in approximately the same number of annual immigrants per value of λ.
Epidemiological parameters		
Probability of becoming infectious	*~Beta(n, 5)*	Where n = number of weeks since exposure. Results in a typical latent period of 3–6 weeks (Figure 2-3, Tinline et al., 2002)
Probability of recovery from exposure	0.002/week	Results in a total recovery rate of approximately 10% (Slate et al., 2014)
Infectious period	1 week	(Hanlon et al., 2007)
Transmission coefficient	λ_1 = 0.035 λ_2 = 0.02	In which λ_1 = transmission rate to raccoons occupying the same cell as the infected raccoon; λ_2 = transmission rate to raccoons occupying any other cell within the infected raccoon's home range (Figures 2-6 – 2-9)
Initial infection time	Year 2, Week 1	
Initial infections	40	Raccoons to be infected initially are randomly selected from non-immune raccoons
Vaccination probability (raccoons at least 52 weeks of age)	Varies	Takes values from 0–80% at intervals of 10%
Vaccination probability (raccoons less than 52 weeks of age)	Vaccination probability / 2	(Beasley et al., 2024)
Immunity duration	Permanent	Vaccine-induced immunity duration is unknown. Previous work has included permanent immunity (e.g. McClure et al., 2020, but see Acheson et al., 2023)
Infection rate of immigrants	Varies	Values include 0, 0.015, 0.03, 0.045, and 0.06

Additional Literature Cited

Acheson, E. S., Viard, F., Buchanan, T., Nituch, L., & Leighton, P. A. (2023). Comparing Control Intervention Scenarios for Raccoon Rabies in Southern Ontario between 2015 and 2025. *Viruses*, *15*(2), Article 2. https://doi.org/10.3390/v15020528

Beasley, E. M., Nelson, K. M., Slate, D., Gilbert, A. T., Pogmore, F. E., Chipman, R. B., & Davis, A. J. (2024). Oral Rabies Vaccination of Raccoons (Procyon lotor) across a Development Intensity Gradient in Burlington, Vermont, USA, 2015–2017. *Journal of Wildlife Diseases*, *60*(1), 1–13. https://doi.org/10.7589/JWD-D-22-00117

Biek, R., Henderson, J. C., Waller, L. A., Rupprecht, C. E., & Real, L. A. (2007). A high-resolution genetic signature of demographic and spatial expansion in epizootic rabies virus. *Proceedings of the National Academy of Sciences*, *104*(19), 7993–7998. https://doi.org/10.1073/pnas.0700741104

Childs, J. E., Curns, A. T., Dey, M. E., Real, L. A., Feinstein, L., Bjørnstad, O. N., & Krebs, J. W. (2000). Predicting the local dynamics of epizootic rabies among raccoons in the United States. *Proceedings of the National Academy of Sciences*, *97*(25), 13666–13671. https://doi.org/10.1073/pnas.240326697

Etherington, T. R., Holland, E. P., & O'Sullivan, D. (2015). NLMpy: A python software package for the creation of neutral landscape models within a general numerical framework. *Methods in Ecology and Evolution*, *6*(2), 164–168. https://doi.org/10.1111/2041-210X.12308

Fournier, A., Fussell, D., & Carpenter, L. (1982). Computer rendering of stochastic models. *Communications of the ACM*, *25*(6), 371–384. https://doi.org/10.1145/358523.358553

Gehrt, S. D., & Prange, S. (2007). Interference competition between coyotes and raccoons: A test of the mesopredator release hypothesis. *Behavioral Ecology*, *18*(1), 204–214. https://doi.org/10.1093/beheco/arl075

Hanlon, C. A., Niezgoda, M., & Rupprecht, C. E. (2007). 5—Rabies in Terrestrial Animals. In A. C. Jackson & W. H. Wunner (Eds.), *Rabies (Second Edition)* (pp. 201–258). Academic Press. https://doi.org/10.1016/B978-012369366-2/50007-5

Hauver, S. A., Gehrt, S. D., Prange, S., & Dubach, J. (2010). Behavioral and genetic aspects of the raccoon mating system. *Journal of Mammalogy*, *91*(3), 749–757. https://doi.org/10.1644/09-MAMM-A-067.1

Hesselbarth, M. H. K., Sciaini, M., With, K. A., Wiegand, K., & Nowosad, J. (2019). landscapemetrics: An open-source R tool to calculate landscape metrics. *Ecography*, *42*(10), 1648–1657. https://doi.org/10.1111/ecog.04617

McClure, K. M., Gilbert, A. T., Chipman, R. B., Rees, E. E., & Pepin, K. M. (2020). Variation in host home range size decreases rabies vaccination effectiveness by increasing the spatial spread of rabies virus. *Journal of Animal Ecology*, *89*(6), 1375–1386. https://doi.org/10.1111/1365-2656.13176

Palmer, M. W. (1992). The Coexistence of Species in Fractal Landscapes. *The American Naturalist*, *139*(2), 375–397. https://doi.org/10.1086/285332

Pitt, J. A., Larivière, S., & Messier, F. (2008). Survival and Body Condition of Raccoons at the Edge of the Range. *The Journal of Wildlife Management*, *72*(2), 389–395. https://doi.org/10.2193/2005-761

Poisot, T., Borregaard, M. K., Catchen, M. D., Schouten, R., & Baudrot, V. (2023). *NeutralLandscapes* (Version 0.1.3) [Julia]. https://docs.ecojulia.org/NeutralLandscapes.jl/dev/

Prange, S., Gehrt, S. D., & Wiggers, E. P. (2003). Demographic factors contributing to high raccoon densities in urban landscapes. *The Journal of Wildlife Management*, 324–333.

Rees, E. E., Pond, B. A., Phillips, J. R., & Murray, D. (2008). Raccoon ecology database: A resource for population dynamics modelling and meta-analysis. *Ecological Informatics*, *3*(1), 87–96. https://doi.org/10.1016/j.ecoinf.2008.01.002

Rees, E. E., Pond, B. A., Tinline, R. R., & Bélanger, D. (2013). Modelling the effect of landscape heterogeneity on the efficacy of vaccination for wildlife infectious disease control. *Journal of Applied Ecology*, *50*(4), 881–891. https://doi.org/10.1111/1365-2664.12101

Sanderson, G. C., & Nalbandov, A. V. (1973). The Reproductive Cycle of the Raccoon in Illinois. *Illinois Natural History Survey Bulletin; v. 031, No. 02*. https://hdl.handle.net/2142/44058

Slate, D., Chipman, R. B., Algeo, T. P., Mills, S. A., Nelson, K. M., Croson, C. K., Dubovi, E. J., Vercauteren, K., Renshaw, R. W., Atwood, T., Johnson, S., & Rupprecht, C. E. (2014). Safety and immunogenicity of Ontario Rabies Vaccine Bait (ONRAB) in the first US field trial in raccoons (Procyon lotor). *Journal of Wildlife Diseases*, *50*(3), 582–595. https://doi.org/10.7589/2013-08-207

Tinline, R., Ball, D., Broadfoot, J., & Pond, B. (2007). The Ontario rabies model. *Queens University, Kingston, Ontario, Canada*.

Tinline, R., Rosatte, R., & MacInnes, C. (2002). Estimating the incubation period of raccoon rabies: A time–space clustering approach. *Preventive Veterinary Medicine*, *56*(1), 89–103. https://doi.org/10.1016/S0167-5877(02)00126-5

911

912

Appendix 3: Supplemental Tables and Figures

E.M. Beasley and T. Poisot

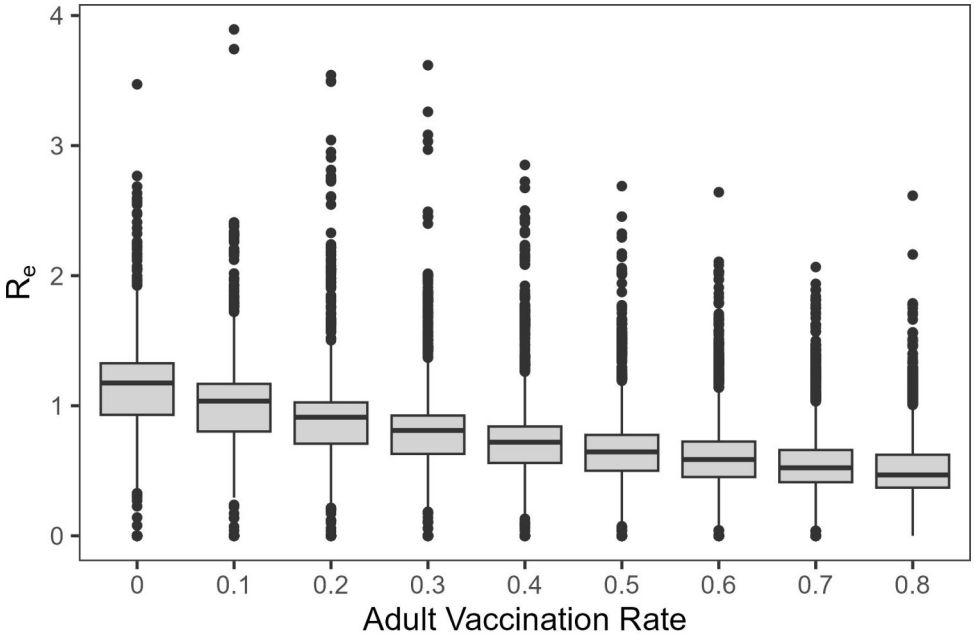

Figure 1. Estimated effective reproduction numbers (R_e) across simulations with varying adult vaccination rates. R_e tended to decrease as the vaccination rate increased, which is expected given the lower proportion of susceptible individuals in the population. Mean estimates of R_e in landscapes with an adult vaccination rate of 0% (1.14) are consistent with empirical estimates (~1–1.2).

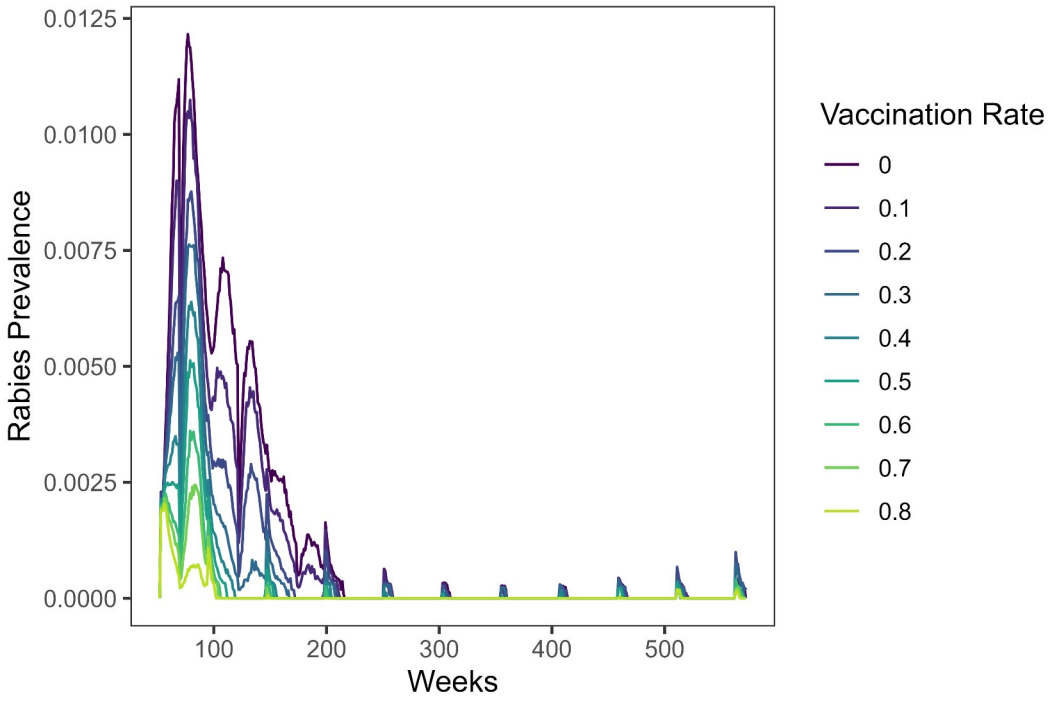

924 **Figure 2.** Average weekly rabies prevalence in simulated raccoon populations with varying adult
925 vaccination rates. Prevalence was generally low in all simulations, and was lower in simulations
926 with higher vaccination rates. Increases in average prevalence beyond week 200 correspond to
927 periods of seasonal immigration in some simulations.

928

929

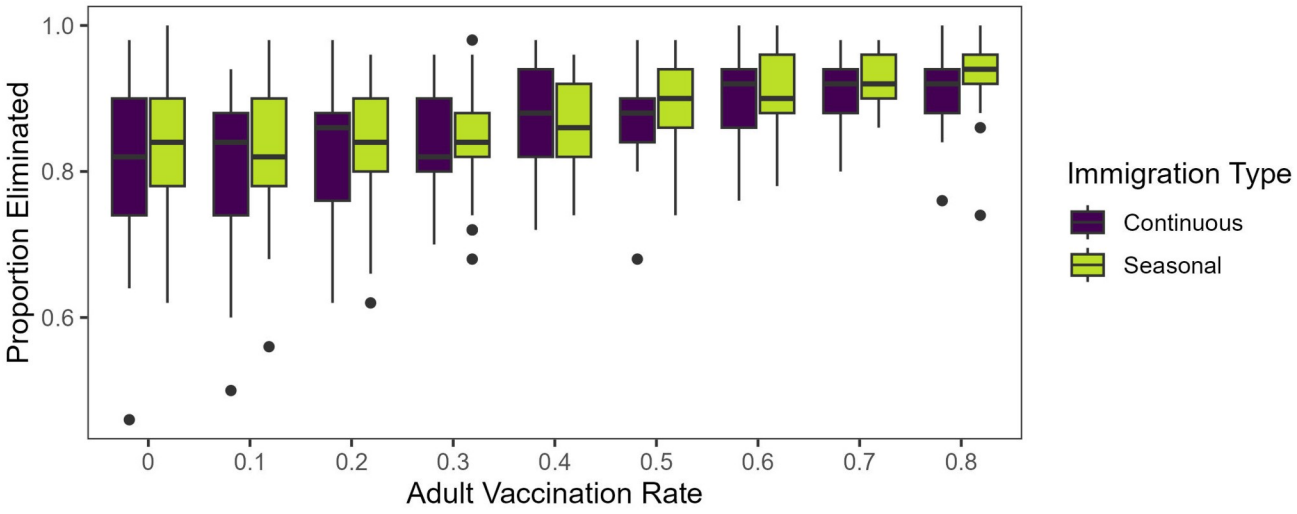

931 **Figure 3.** Mean proportion of simulated rabies outbreaks eliminated by adult vaccination rate
932 and immigration type. Among simulations with the same vaccination rate, simulations with
933 continuous immigration were slightly less likely to achieve rabies elimination than simulations
934 where immigration was restricted to a specific part of the year. This effect tended to be more
935 pronounced in landscapes with adult vaccination rates of at least 50%.

936

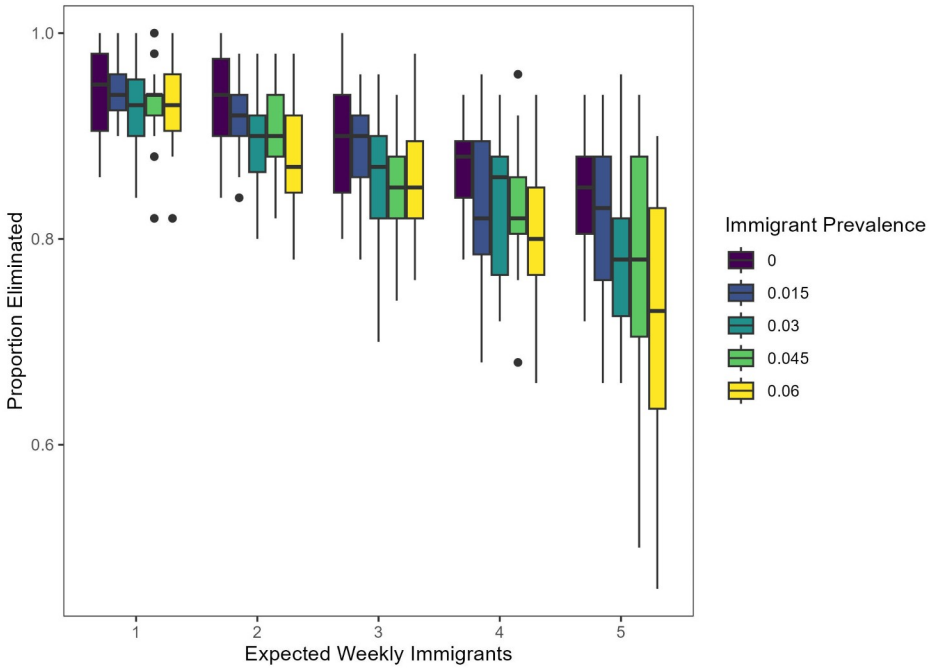

Figure 4. Proportion of simulated rabies outbreaks eliminated across simulations with varying values of expected weekly immigrants and the disease prevalence of immigrants. Elimination was least likely to be achieved when immigration rate and immigrant prevalence were both high. Effects of immigrant prevalence tended to be more pronounced in simulations with higher immigration rates.

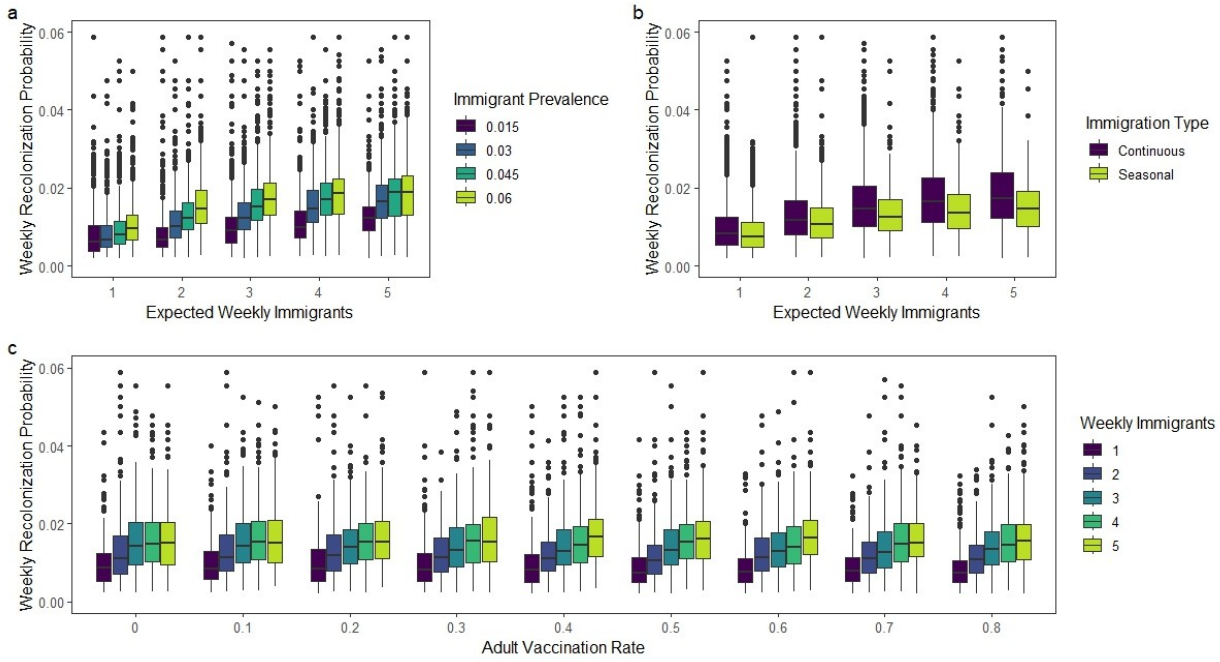

944

945 **Figure 5.** Effects of immigration variables on the weekly probability of rabies recolonization
946 after the initial rabies elimination. Recolonization probability increased with immigration rate (a,
947 b), defined as the expected number of weekly immigrants, and rabies prevalence of immigrants
948 (a). Recolonization was also more likely when immigration occurred continuously rather than
949 seasonally (b). Vaccination rates had no clear effect on recolonization probability (c).

950

951

952

953

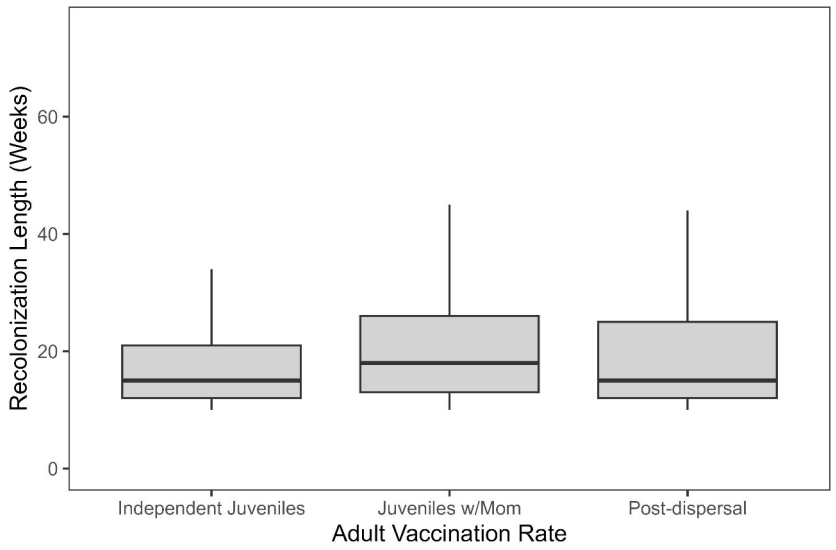

954 **Figure 6.** Mean duration of recolonization events, in weeks, based on the timing of the
955 reinfection event. There were no clear differences in duration between the three time periods.
956 Most recolonization events lasted less than one year. Outliers removed for clarity.

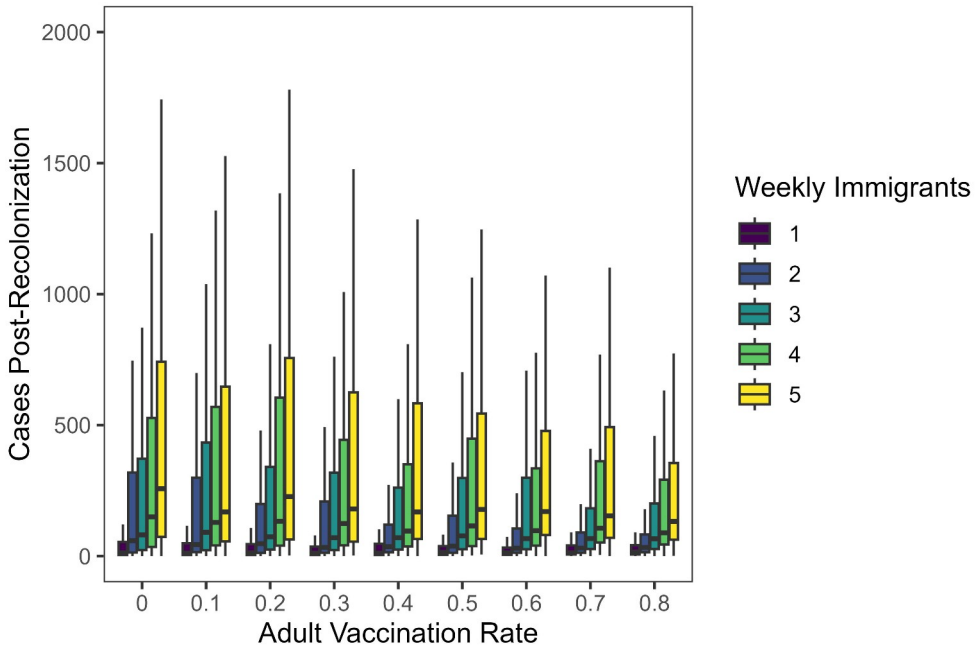

958 **Figure 7**. Mean cases after rabies recolonization. Cases after a recolonization event were higher
959 in simulations with higher immigration rates and lower in simulations with higher vaccination
960 rates.